



Review

Perry Disease: Current Outlook and Advances in Drug Discovery Approach to Symptomatic Treatment

Zbigniew Gajda [†] , Magdalena Hawrylak [†], Jadwiga Handzlik and Kamil J. Kuder ^{*†}

Department of Technology and Biotechnology of Drugs, Faculty of Pharmacy, Jagiellonian University Medical College in Kraków, Medyczna 9, 30-688 Krakow, Poland; zbigniew.gajda@student.uj.edu.pl (Z.G.); magdalena.hawrylak@student.uj.edu.pl (M.H.); j.handzlik@uj.edu.pl (J.H.)

* Correspondence: kamil.kuder@uj.edu.pl

[†] These authors contributed equally to this work.

Abstract: Perry disease (PeD) is a rare, neurodegenerative, genetic disorder inherited in an autosomal dominant manner. The disease manifests as parkinsonism, with psychiatric symptoms on top, such as depression or sleep disorders, accompanied by unexpected weight loss, central hypoventilation, and aggregation of DNA-binding protein (TDP-43) in the brain. Due to the genetic cause, no causal treatment for PeD is currently available. The only way to improve the quality of life of patients is through symptomatic therapy. This work aims to review the latest data on potential PeD treatment, specifically from the medicinal chemistry and computer-aided drug design (CADD) points of view. We select proteins that might represent therapeutic targets for symptomatic treatment of the disease: monoamine oxidase B (MAO-B), serotonin transporter (SERT), dopamine D₂ (D₂R), and serotonin 5-HT_{1A} (5-HT_{1A}R) receptors. We report on compounds that may be potential hits to develop symptomatic therapies for PeD and related neurodegenerative diseases and relieve its symptoms. We use Phase pharmacophore modeling software (version 2023.08) implemented in Schrödinger Maestro as a ligand selection tool. For each of the chosen targets, based on the resolved protein–ligand structures deposited in the Protein Data Bank (PDB) database, pharmacophore models are proposed. We review novel, active compounds that might serve as either hits for further optimization or candidates for further phases of studies, leading to potential use in the treatment of PeD.



Citation: Gajda, Z.; Hawrylak, M.; Handzlik, J.; Kuder, K.J. Perry Disease: Current Outlook and Advances in Drug Discovery Approach to Symptomatic Treatment. *Int. J. Mol. Sci.* **2024**, *25*, 10652. <https://doi.org/10.3390/ijms251910652>

Academic Editor: Antonietta Bernardo

Received: 10 July 2024

Revised: 27 August 2024

Accepted: 31 August 2024

Published: 3 October 2024



Copyright: © 2024 by the authors. Licensee MDPI, Basel, Switzerland. This article is an open access article distributed under the terms and conditions of the Creative Commons Attribution (CC BY) license (<https://creativecommons.org/licenses/by/4.0/>).

Keywords: Perry disease; neurodegeneration; rare disease; pharmacophore; MAO-B; SERT; serotonin 5-HT_{1A} receptor; dopamine D₂ receptor; polypharmacology; multi target drug

1. Introduction

1.1. Neurodegeneration and Inflammation

Neurodegenerative diseases (NDDs) constitute a diverse set of neurological disorders that impact millions of people globally, leading to the gradual deterioration of the nervous system. The vast spectrum of NDDs includes Alzheimer’s disease (AD), Parkinson’s disease (PD), primary tauopathies, frontotemporal dementia (FTD), amyotrophic lateral sclerosis (ALS), synucleinopathies (i.e., Lewy body dementia [LBD] and multisystem atrophy [MSA]), Huntington’s disease (HD) and related polyglutamine (polyQ) diseases (including spinocerebellar ataxias [SCA]), prion disease (PrD), traumatic brain injury (TBI), chronic traumatic encephalopathy (CTE), stroke, spinal cord injury (SCI), and multiple sclerosis (MS) [1].

Worldwide, NDDs impact millions of individuals. The two most prevalent NDDs are PD and AD. A 2024 report from the Alzheimer’s Disease Association estimated that as many as 6.9 million patients in the USA may suffer from AD [2]. On the other hand, the Parkinson’s Foundation estimates that approximately one million patients in the USA are diagnosed with PD [3].

NDDs share many fundamental processes associated with progressive neuronal dysfunction and death, including oxidative stress, programmed cell death, proteotoxic

stress, and its attendant abnormalities in the ubiquitin–proteasomal and autophagosomal/lysosomal systems, and neuroinflammation [4]. These processes cause the deterioration of neural networks in either the central (CNS) or peripheral (PNS) nervous system, which ultimately results in impaired memory, cognition, behavior, sensory perception, and/or motor function [1]. Consequently, the clinical presentations of NDDs can be used to categorize them broadly, with the most common types being extrapyramidal and pyramidal movement disorders, as well as cognitive or behavioral disorders. Most patients have a combination of clinical features, with very few having pure syndromes. Hence, neuropathological evaluation during the autopsy constitutes the gold standard for diagnosis, as specific protein accumulations and anatomic vulnerability are typically used to define NDDs [4].

While several medications are currently approved to treat NDDs, most of them provide only symptomatic treatment. The blood–brain barrier’s (BBB’s) limiting properties, which prevent nearly 99% of all xenobiotics from entering the brain, are the main cause of the lack of pathogenesis-targeting treatments [5].

1.2. Rare Diseases

A rare or orphan disease is a medical condition that affects a small percentage of the population [6]. As of 2021, rare diseases affect more than 470 million people worldwide—approximately 1/16 of the global population [7]. Despite significant advances in research, which have enhanced our understanding of the molecular foundations of these diseases and the availability of regulatory and economic incentives to speed up the development of treatments, most rare diseases still lack approved therapies [8]. One of the primary challenges in treating these conditions is the lack of standardized terminology and definitions, which hampers accurate diagnosis, disease classification, and the development of targeted treatments. Regulatory agencies provide incentives for pharmaceutical companies to develop therapies for these conditions, known as orphan drugs [9]—e.g., the Food and Drug Administration (FDA) grants orphan drugs sponsors tax credits for qualified clinical trials, exemption from user fees, or a potential seven years of market exclusivity after approval [10,11]. Still, less than 10% of patients with rare diseases receive treatments specifically tailored to their conditions [7]. Developing orphan drugs involves various strategies, including protein replacement therapies, small-molecule therapies, gene and cell therapies, and drug repurposing. Each approach comes with its strengths and limitations, and the process is further complicated by challenges in clinical trials, such as difficulties in patient recruitment, incomplete understanding of disease mechanisms, increased genetic heterogeneity, lack of animal models, and ethical concerns, particularly in pediatric cases. Additionally, the legislative procedure does not differ significantly from registering medicines for more common diseases—it adds another level of complexity to developing treatment for rare diseases, but on the other hand, grants necessary safety to patients upon releasing the drug to the market. Overcoming these barriers requires a collaborative effort involving academic institutions, industry, patient advocacy groups, and regulatory bodies to ensure that advances in rare disease research can be effectively translated into viable treatments [8].

1.3. Perry Disease

Perry disease (PeD) is a rare, genetic NDD inherited in an autosomal dominant manner. The disease manifests as parkinsonism, with psychiatric symptoms on top, such as depression or sleep disorders, and is accompanied by unexpected weight loss, central hypoventilation, and aggregation of DNA-binding protein (TDP-43) in the brain [12,13].

The cause of PeD is a mutation in the dynactin I gene (DCTN1), which is responsible for encoding the p150 subunit. Dynactin is a motor protein associated with axonal transport, while the aforementioned subunit constitutes a microtubule-binding site, an important feature of dynactin action [12]. Up until the fall of 2023, over 30 families with PeD have been reported [14]. Other than the “classic” type of disease, distinct phenotypes are recognized and classified as PeD [12].

1.4. Perry Disease Treatment

Due to the genetic cause, no causal treatment for PeD is currently available. Therefore, for patients suffering from this condition, the only way to improve their quality of life is through symptomatic therapy [15].

In this context, lines of evidence indicate levodopa (L-DOPA) [16–18], monoamine oxidase B (MAO-B) inhibitors [17], dopamine agonists [19,20], L-DOPA decarboxylase inhibitors [21], anticholinergics [17] or, very generally, wide-ranging groups of antidepressants, e.g., selective serotonin reuptake inhibitors (SSRIs) and tricyclic antidepressants (TCAs) [17,18], as helpful for PeD patients. Yet, to the best of our knowledge, no specific treatment for PeD has been either proposed or approved by any of the relevant legislative bodies.

2. Aim of Work

This work aims to review the latest data on potential PeD treatment, specifically from the medicinal chemistry and computer-aided drug design (CADD) points of view. Based on the medication therapies described so far and our knowledge, we have selected proteins that might represent therapeutic targets for the symptomatic treatment of the disease. The targets of focus in this work break down as follows: enzymes—MAO-B, sodium-dependent serotonin transporter (SERT); receptors—dopamine D₂ (D₂R) and serotonin 5-HT_{1A} (5-HT_{1A}R). We will report on compounds that may be potential hits for developing symptomatic therapies for PeD and related NDDs, for relieving symptoms.

Since the selected proteins have been widely explored as potential therapeutic targets and, consequently, the vast chemical space of the ligands has been proposed for them, in the present work, we have mostly focused on the structures published since 2020, which, in preliminary biological studies, display expected activity toward the objectives of the review.

To narrow down the search area, we use the pharmacophore modeling software Phase implemented in Schrödinger Maestro [22,23]. For each of the chosen targets, based on the resolved protein–ligand structures deposited in the Protein Data Bank (PDB) database (Table 1) [24], pharmacophore models are proposed using the default settings, except for SERT and 5-HT_{1A}R, for which the following features have been manually added: positive ionic, aromatic ring, and hydrophobic or another aromatic ring (respectively). In the next step, the appropriately filtered (parameters given at the beginning of each section) ligand databases downloaded from ChEMBL [25,26] are screened using the proposed model. Up to the 10 most favorable results, in our opinion, are then tabulated (ranked by the Phase Screen Score value) and shortly described. The majority of the compounds from the screening results exhibit all the pharmacophore model features (for their respective target), except the D₂R ligands, which mostly lack one of the aromatic features (the raw screening results are available as Supplementary Data).

Table 1. Biological targets and their Protein Data Bank (PDB) entries used to develop the pharmacophore models.

Biological Target ¹	PDB ID ²	Ligand ³	Ligand Type ⁴
MAO-B	2V5Z [27]	Safinamide	Antagonist
SERT	6AWO [28]	Sertraline	Antagonist
D ₂ R	8IRS [29]	Rotigotine	Agonist
5-HT _{1A} R	7E2Y [30]	Serotonin	Endogenous agonist

¹ Targets include monoamine oxidase B (MAO-B), sodium-dependent serotonin transporter (SERT), dopamine D₂ receptor (D₂R), and serotonin 1A receptor (5-HT_{1A}R). ² PDB Identification Code (PDB ID) denotes a unique code under each molecular model deposited in the PDB. ³ Ligand denotes a small molecule bound to the target's binding pocket. ⁴ Ligand type denotes the pharmacological type of the bound ligand.

3. Results

3.1. Enzymes

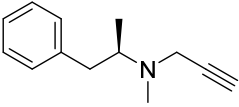
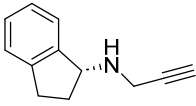
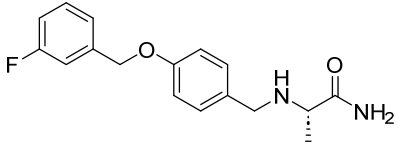
3.1.1. Monoamine Oxidase B

Monoamine oxidase (MAO) is a mitochondrial enzyme that catalyzes the oxidative deamination of various monoamines. It plays a significant role in the metabolism of released neurotransmitters and the detoxification of a wide variety of endo- and exogenous amines. Two isoforms of this enzyme that are approximately 70% identical to each other are known—monoamine oxidase A (MAO-A) and MAO-B. MAO-A is the predominant form in the gastrointestinal tract, placenta, and heart, while MAO-B is prevalent in brain glial cells and platelets. Regardless of the isoform or occurrence, both are covalently bound to flavin adenine dinucleotide (FAD) [31,32].

Many studies suggest that MAO-B participates in the pathomechanism of NDDs associated with aging. Unlike most enzymes, its activity does not decrease but increases linearly beyond 60 years of age. The enzyme is also considered to be involved in the formation of free radicals. Due to its function, MAO-B is also the main enzyme involved in dopamine metabolism, therefore playing a key role in the pathophysiology of PD. Hence, MAO-B inhibitors in combination with levodopa have found use in PD treatment [33].

MAO-B inhibitors have excellent efficacy and are safe for use both in the initial stages of PD and (as adjunctive therapy) in its advanced form. Longer exposure to MAO-B inhibitors results in a lower demand for levodopa and slower disease progression. Drugs currently approved for therapy include irreversible MAO-B inhibitors selegiline and rasagiline and the reversible inhibitor safinamide (Table 2) [34].

Table 2. Overview of currently utilized MAO-B inhibitors.

Compound ¹	ChEMBL ID ²	Structure	MAO-B IC ₅₀ [nM] ³
Selegiline	CHEMBL972		36.0 [35]
Rasagiline	CHEMBL887		15.4 [36]
Safinamide	CHEMBL396778		29.0 [37]

¹ MAO-B inhibitors: selegiline, rasagiline, and safinamide, including ² their unique ChEMBL database Identification Code (ChEMBL ID) and ³ half maximal inhibitory concentration (IC₅₀), respectively.

Out of the structure of MAO-B complexed with safinamide (inhibitor; PDB ID: 2V5Z), a pharmacophore model was proposed (Figures 1 and 2, Table 3).

Table 3. Distances (in Å) between the proposed MAO-B pharmacophore model features.

Pharmacophore Features	D4	H5	R7	R8
R8	5.14	7.50	6.38	
R7	10.94	2.76		
H5	12.51			
D4				

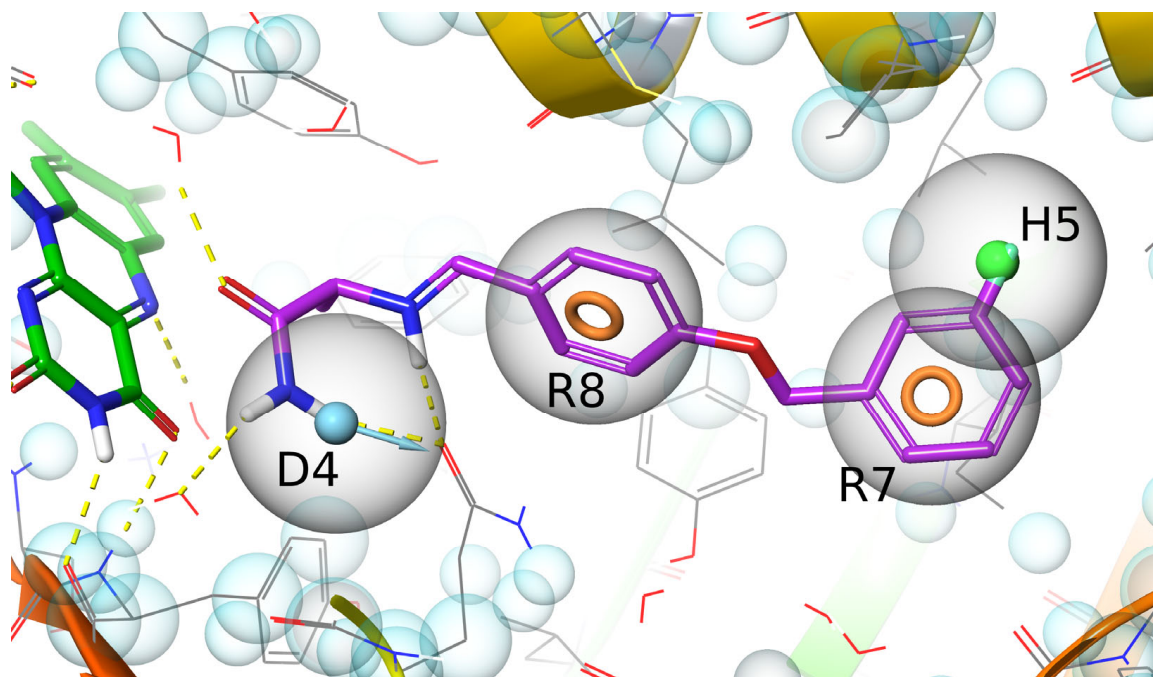


Figure 1. Safinamide (purple) complexed with MAO-B (gray) with, superimposed, the proposed pharmacophore model (balls and toruses). Dashed lines denote hydrogen bonds (yellow). Balls denote hydrogen bond donor feature (D, blue, arrow indicates bond direction) and hydrophobic feature (H, green), and toruses denote aromatic features (R, orange). Blue spheres denote excluded volumes. On the left, the flavin adenine dinucleotide (FAD) structure is visible (green).

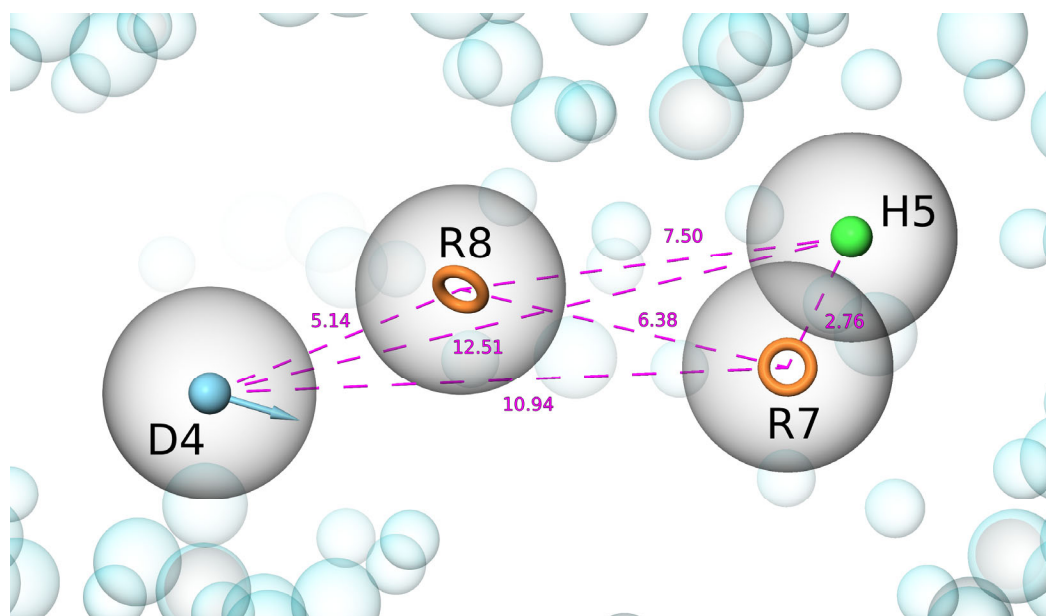


Figure 2. Proposed MAO-B pharmacophore model derived from the 2V5Z structure (balls and toruses). Balls denote hydrogen bond donor feature (D, blue, arrow indicates bond direction) and hydrophobic feature (H, green), and toruses denote aromatic features (R, orange). Dashed purple lines denote distances between features, with measurements in Å written beside them. Blue spheres denote excluded volumes.

3.1.2. 2V5Z (Monoamine Oxidase B) Pharmacophore Screening

In the ChEMBL database, we queried for molecules exhibiting a half maximal inhibitory concentration (IC_{50}) ≤ 100 nM in human MAO-B inhibition in assays published in 2020 and later, then conducted pharmacophore-based ligand screening using the model proposed by the Phase module (Table 4).

Table 4. MAO-B pharmacophore screening results, including up to 10 hit molecules, excluding well-established medicines and pharmacological tools.

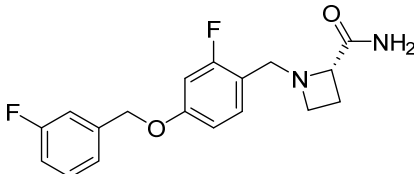
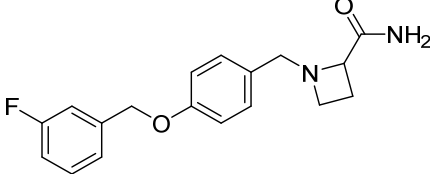
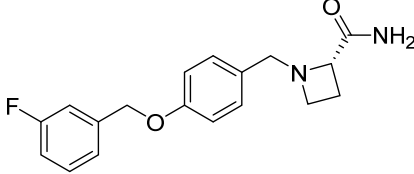
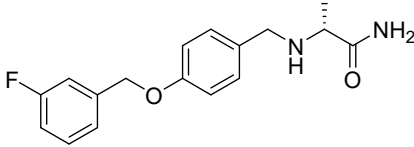
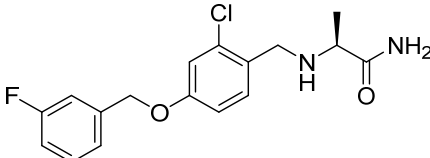
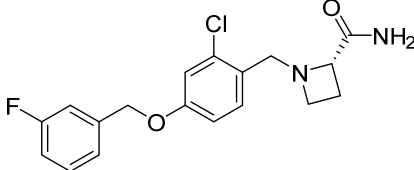
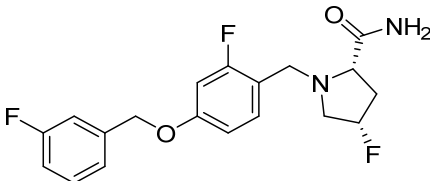
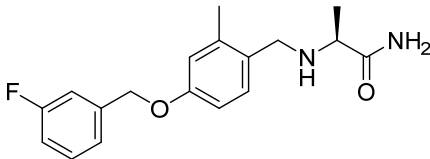
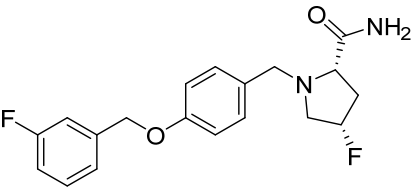
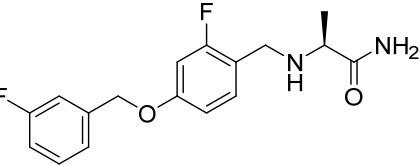
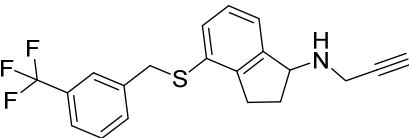
Compound	ChEMBL ID	Structure	PhaseScreenScore	MAO-B IC_{50} [nM]
M1	CHEMBL4749026		2.203314	26.0 [38]
M2	CHEMBL4792241		2.051776	46.0 [38]
M3	CHEMBL4747396		2.051776	21.0 [38]
Safinamide	CHEMBL396778		2.048958	25.0 [38]
M4	CHEMBL4750661		1.941374	28.0 [38]
M5	CHEMBL4763805		1.923999	35.0 [38]
M6	CHEMBL5077617		1.857744	30.0 [39]
M7	CHEMBL4752402		1.799135	69.0 [38]

Table 4. Cont.

Compound	ChEMBL ID	Structure	PhaseScreenScore	MAO-B IC ₅₀ [nM]
M8	CHEMBL5083414		1.715590	19.0 [39]
M9	CHEMBL4743831		1.708420	61.0 [38]
M10	CHEMBL4860050		1.569462	4.7 [40]

Seven out of ten compounds screened were published within the same work [38] focusing on fragment-based drug design (FBDD) for the discovery of selective MAO-B inhibitors. In this study, a steric clash-induced binding allosteric (SCIBA) strategy was used, in which the fragment entering the collision with the non-biological target protein—in this case, MAO-A—was the pharmacophore element. This arrangement provided greater selectivity to the correct target, MAO-B. Based on the structure of safinamide, the researchers found the fragment that was most sterically unfavorable for MAO-A (1-fluoro-3-phenoxyethylbenzene) and looked for combinations with fragments that could match the MAO-B active site, e.g., safinamide forms hydrophobic interactions with Phe103, Leu164, Leu167, Leu171, Ile199 and Tyr398, and it forms a hydrogen bond with Gln206. In the case of MAO-A, the binding site is curved so that safinamide collides sterically with Phe208. This results in an unfavorable conformational change of safinamide and a lack of hydrogen bonding with Gln215, which significantly worsens the affinity for this enzyme [38]. Based on these observations, a set of (S)-2-(benzylamino)-propanamide derivatives were designed, synthesized, and biologically evaluated. Two series of compounds were obtained. The first series included compounds **M4**, **M7**, and **M9**—and it was devoid of heterocyclic moieties (except for CHEMBL4759613 containing morpholine, not listed herein). The second series containing azacyclic amides included **M1**, **M2**, **M3**, and **M5**. Modifications of safinamide involving the addition of fluoride or a methyl group into central benzyl position 2 achieved strong inhibitory activity against MAO-B. The best activity among those reported was achieved by the **M4** containing chloride substituent in position 2 of the central benzene ring, which ranked fifth in our screening [38].

Studies of a series of azacyclic amides also showed that the presence of a chiral group is beneficial for MAO-B inhibition, i.e., the MAO-B inhibitory activity of S-enantiomer **M3** (IC₅₀ = 21 nM) was superior when compared to its racemate **M2** (IC₅₀ = 46 nM) and similar to that of safinamide. **M1** and **M5** with electron-acceptor substituents (-F or -Cl) also showed strong inhibitory activity (IC₅₀ = 26 nM and 35 nM, respectively) [38]. The strongest activity of all seven compounds was shown by **M3**, which was ranked third in our screening. **M1**, with slightly less MAO-B inhibitory activity, was identified as the best fit by our model [38].

M6 and **M8** were obtained using the FBDD method, based on a previously described series of (S)-2-(benzylamino)propanamide derivatives, which led them to conclude that the chiral amide group located at position 2 of the azetidine ring was important for MAO-B inhibition [39]. The modifications involved the introduction of chiral fluorinated pyrrolidine derivatives into a new series of compounds. **M8** appeared to be the most active, having

a chiral fluorine atom in position 4 of the pyrrolidine ring. **M6**, obtained by introducing a fluorine atom into position 2 of the benzene ring, also showed good MAO-B inhibitory activity. Both compounds also showed remarkably high selectivity for MAO-B over MAO-A (**M6**, MAO-A IC_{50} = 29360.0 nM, **M8**, IC_{50} = 46365.0 nM) [39].

Last in order, according to our screening, **M10** was derived from the study, which was a continuation of the search for MAO-B inhibitors using FBDD methods [40]. Previously, the researchers combined rasagiline with a hydrophobic molecule, resulting in selective compounds with promising activities against MAO-B, and in the study described here, the linkers and hydrophobic groups were modified to yield compounds with a 1-(prop-2-yn-1-ylamino)-2,3-dihydro-1H-inden-4-thiol scaffold [40].

M10 with a 3-(trifluoromethyl)benzyl substituent had very high activity (IC_{50} = 4.7 nM) and was highly selective for MAO-B over MAO-A (Selectivity Index [SI] = MAO-A IC_{50} /MAO-B IC_{50} = 1641.3). These were better results than those achieved by rasagiline and safinamide in the same study. The only compound with even higher activity against MAO-B and selectivity, as obtained in this study, had a 1-methyl-3-propylbenzene fragment instead of a 1-ethyl-3-(trifluoromethyl)benzene fragment (IC_{50} = 0.35 nM, SI = 14162.9) [40].

In light of this review, it can be deduced that compounds containing, from the left, a 1-fluoro-3-((p-tolyloxy)methyl)benzene fragment linked to an amine or azacyclic ring and an amide group (located on the right side of the compound) with halogen substituents or a methyl group at position 2 of the central aromatic ring have the potential to be potent MAO-B inhibitors. Further, the chirality of the halogen group on the azacyclic ring is of relevance to SAR for the series of described compounds. Last but not least, the (2,3-dihydro-1H-inden-4-yl)(3-(trifluoromethyl)benzyl)sulfane fragment linked to the amine-alkyne fragment is a promising framework for study and further modification.

3.1.3. Sodium-Dependent Serotonin Transporter

SERT is a protein located in presynaptic neurons. The raphe nuclei's presynaptic neurons release serotonin, which activates the limbic system. Then, serotonin attaches itself to postsynaptic serotonin receptors, which are mostly found in limbic regions like the nucleus accumbens, dorsal striatum, hippocampal regions, and cortex. One of the processes for taking the neurotransmitter out of the synaptic cleft is serotonin reuptake, which is facilitated by SERT (Figure 3) [41].

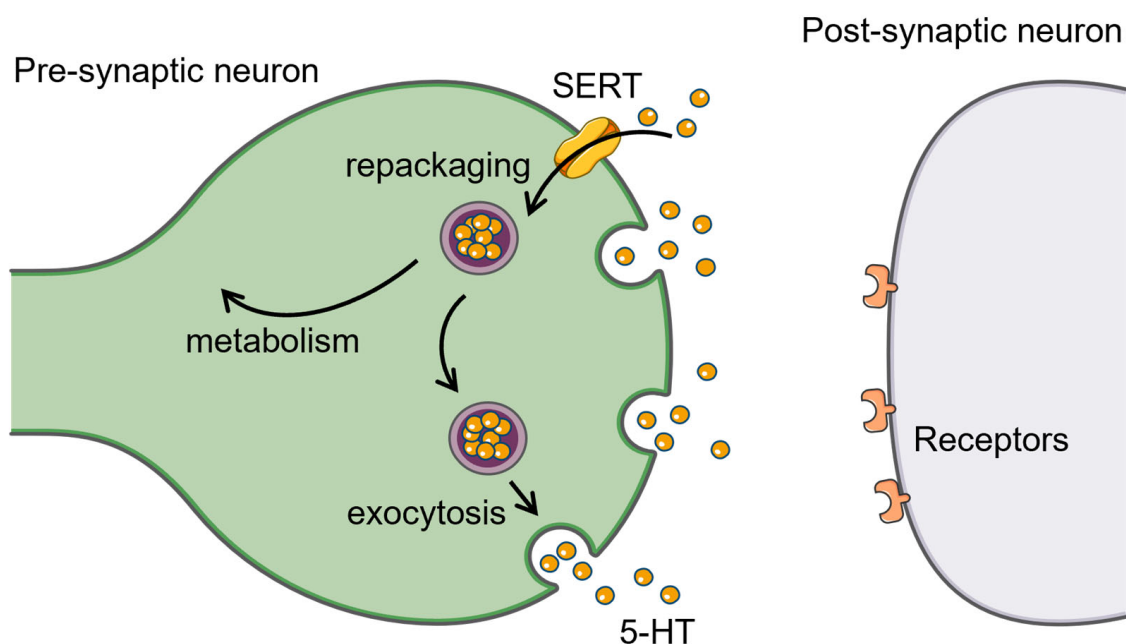


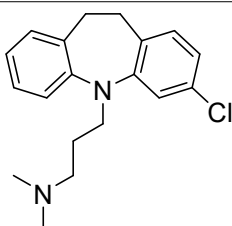
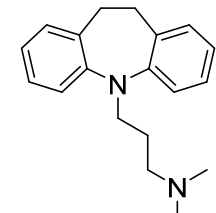
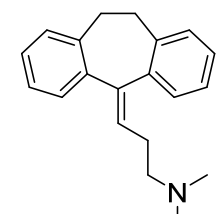
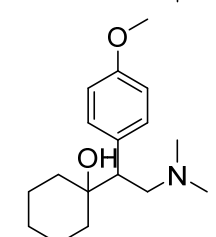
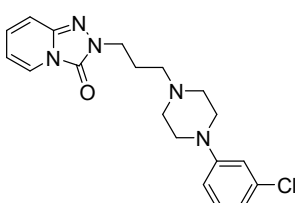
Figure 3. Model of a serotonergic synapse. SERT facilitates serotonin (5-HT, orange spheres) reuptake. Adapted from [42].

Serotonin is related to the regulation of social behavior and emotional responses. Disturbances in serotonin transmission are related to depressive symptoms such as feelings of profound sadness, worthlessness, low self-esteem, suicidal thoughts, and lowered cognitive abilities [41]. Multiple medications achieve an increase in the serotonin concentration in the synaptic cleft by stabilizing the inactive state of SERT, thereby having an antidepressant effect [43]. While serotonin does not play much of a role in PD motor symptoms, serotonergic dysfunction is relevant to PD nonmotor symptoms, like depression, fatigue, weight changes, and visual hallucinations. While the first two are related to inhibition, the latter, on the contrary, is related to an increase in serotonergic transmission [44]. Antidepressants can alleviate them all, but the data on reducing psychotic symptoms are of poor quality [45]. Numerous antidepressants possess SERT activity as well (Table 5) [46].

Table 5. Well-known SERT inhibitors and their inhibitory potencies. The SERT inhibition values were obtained from [26].

Drug Class	Compound	Structure	SERT IC ₅₀ [nM]
SSRI ¹	Paroxetine		0.56
SSRI	Fluoxetine		12.6
SSRI	Sertraline		0.19
SSRI	Citalopram		5.81
SSRI	Fluvoxamine		3.8

Table 5. Cont.

Drug Class	Compound	Structure	SERT IC ₅₀ [nM]
TCA ²	Clomipramine		70.0
TCA	Imipramine		29.0
TCA	Amitriptyline		1.661
SNRI ³	Venlafaxine		20.0
SARI ⁴	Trazodone		192.0

¹ Selective serotonin reuptake inhibitor (SSRI). ² Tricyclic antidepressant (TCA). ³ Serotonin–norepinephrine reuptake inhibitor (SNRI). ⁴ Serotonin antagonist and reuptake inhibitor (SARI).

Out of the structure of SERT complexed with sertraline (inhibitor; PDB ID: 6AWO), a pharmacophore model was proposed (Figures 4 and 5, Table 6).

Table 6. Distances (in Å) between the proposed SERT pharmacophore model features.

Pharmacophore Features	H1	P2	R3
R3	2.50	3.77	
P2	2.81		
H1			

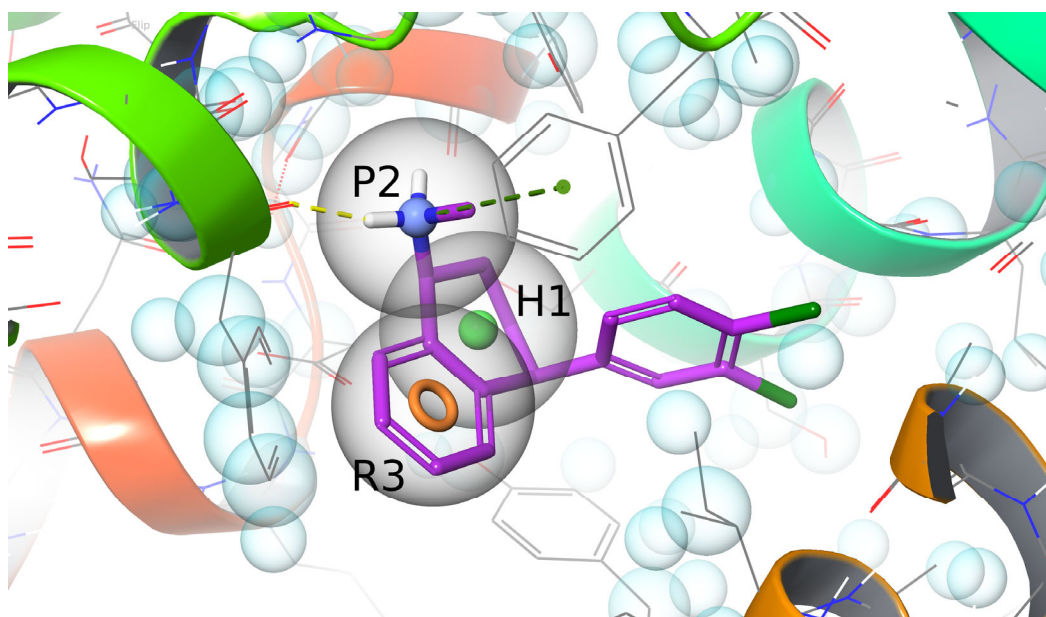


Figure 4. Sertraline (purple) complexed with SERT (gray) superimposed with the proposed pharmacophore model (balls and torus). Dashed lines denote hydrogen bond (yellow) and π -cation interaction (green). Balls denote positive ionic feature (P, blue), hydrophobic feature (H, green) and torus denotes aromatic feature (R, orange). Blue spheres denote excluded volumes.

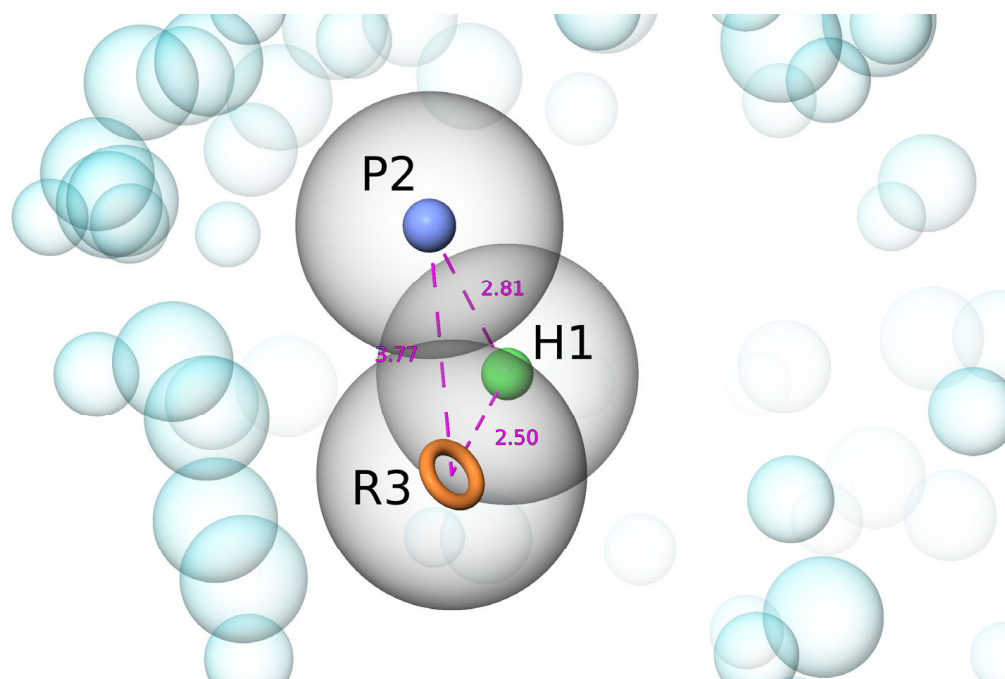


Figure 5. Proposed SERT pharmacophore model derived from the 6AWO structure (balls and torus). Balls denote positive ionic feature (P, blue) and hydrophobic feature (H, green), and torus denotes aromatic feature (R, orange). Dashed purple lines denote distances between features, with measurements in Å written beside them. Blue spheres denote excluded volumes.

3.1.4. 6AWO (Sodium-Dependent Serotonin Transporter) Pharmacophore Screening

In the ChEMBL database, we queried for molecules exhibiting an $IC_{50} \leq 100$ nM in human SERT inhibition in assays published in 2020 and later, then conducted pharmacophore-based ligand screening using the model proposed by the Phase module (Table 7).

Table 7. SERT pharmacophore screening results, including all the output molecules, since the screening results contain less than 10 hit molecules.

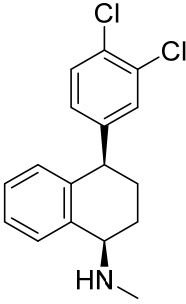
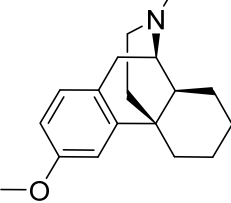
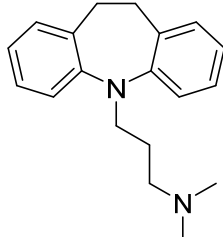
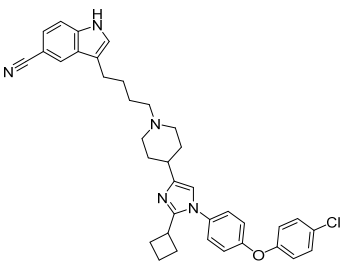
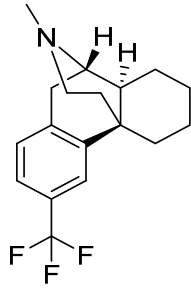
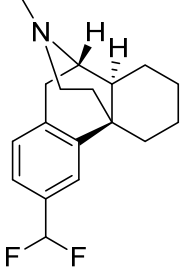
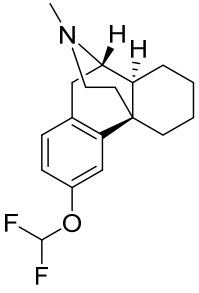
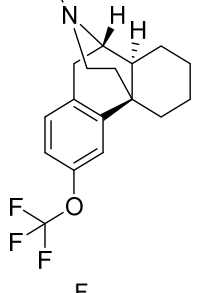
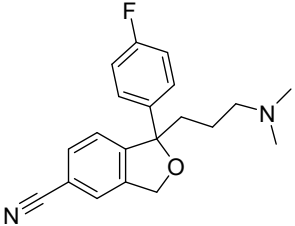
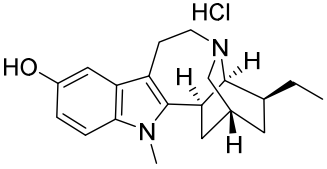
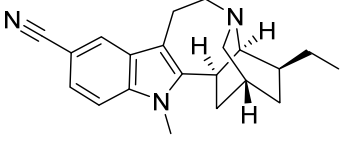
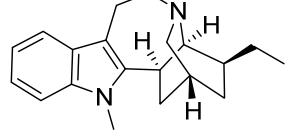
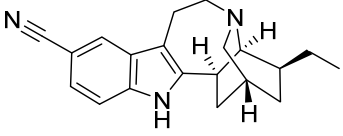
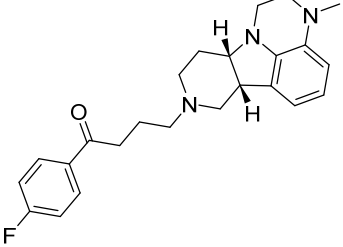
Compound	ChEMBL ID	Structure	PhaseScreenScore	SERT IC ₅₀ [nM]
Sertraline	CHEMBL809		1.963006	0.19 [47]
Dextromethorphan	CHEMBL206132		1.368854	56.0 [48]
Imipramine	CHEMBL11		1.284248	29.0 [47]
S1	CHEMBL5175011		1.199585	7.47 [49]
S2	CHEMBL5086545		0.924859	60.0 [48]
S3	CHEMBL5081803		0.924859	24.0 [48]

Table 7. Cont.

Compound	ChEMBL ID	Structure	PhaseScreenScore	SERT IC ₅₀ [nM]
S4	CHEMBL5093316		0.924859	55.0 [48]
S5	CHEMBL5078388		0.924859	31.0 [48]
Citalopram	CHEMBL549		0.751749	5.81 [50]
S6	CHEMBL5207764		0.584015	59.0 [51]
S7	CHEMBL5188930		0.584015	5.1 [51]
S8	CHEMBL5201219		0.584015	80.0 [51]
S9	CHEMBL5175119		0.583134	26.0 [51]
Lumateperone	CHEMBL3306803		0.490147	3.3 [52]

Except for established, well-known medicines, the screening output described herein contained compounds from three separate studies.

As a novel compound with the highest PhaseScreenScore, there appeared **S1** [49], developed in a study exploring a novel dual receptor for advanced glycation end products (RAGE)/SERT inhibitors for potential application in treating co-morbid AD and depression. Combining such dual inhibition could be beneficial in both conditions, since RAGE facilitates β -amyloid neuronal damage, and its blockade can notably prevent β -amyloid-induced neurotoxicity. The authors based their novel molecules on fusing vilazodone and azeliragon structures: SERT and RAGE inhibitors, respectively (Table 8). Analysis of the potential binding modes of azeliragon to RAGE and vilazodone to SERT showed that, between the aminoalkyl azeliragon moiety and benzofuran vilazodone moiety and their targets, there exists an adjacent pocket. Additionally, the imidazole azeliragon moiety and benzofuran vilazodone moiety (both aromatic heterocycles) could form bonds and interactions with their respective targets, which signifies that central aromatic heterocycles are common, crucial pharmacophoric features in these compounds. Based on these findings, the key pharmacophore structures of both compounds were fused [49].

Firstly, the synthesized chimeric **S10** exhibited some inhibitory potential on both RAGE and SERT, without inheriting vilazodone's partial agonism toward 5-HT_{1A}R. Sadly, it exhibited serious cytotoxicity (which was the reason azeliragon was withdrawn from phase III clinical trials). Because of that, structural modifications were proposed to improve its bioactivity and safety.

Out of pyrazole, phenylimidazole, and thiazole, the only central heterocyclic moiety that preserved the RAGE and SERT activities was the thiazole; therefore, **S10** and **S11** were subjected to further modifications. It is worth noting that the thiazole derivatives preserved dual inhibition better than the pyrazole or benzimidazole derivatives, and the imidazole derivatives displayed stronger SERT inhibition than the thiazole derivatives.

Table 8. Notable compounds explored in the dual receptor for advanced glycation end products (RAGE)/SERT inhibitors study [49].

Compound	ChEMBL ID	Structure	RAGE IC ₅₀ [nM]	SERT IC ₅₀ [nM]
Azeliragon	CHEMBL3989929		13,470	>3000
Vilazodone	CHEMBL439849		>200,000	0.40
S1	CHEMBL5175011		8290.0	7.47

Table 8. Cont.

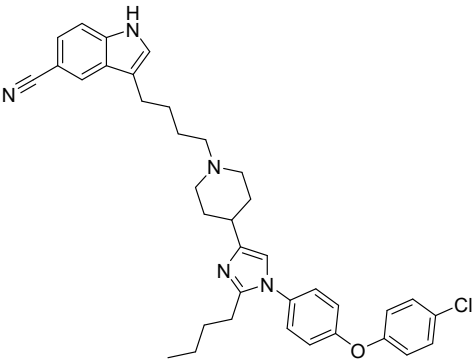
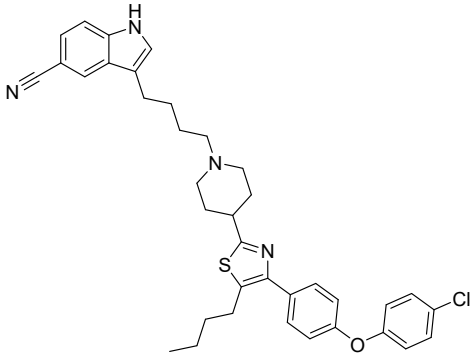
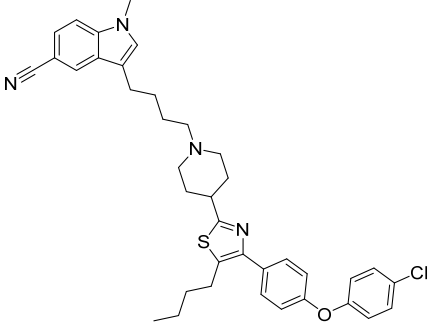
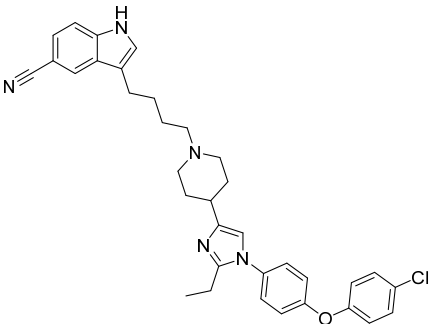
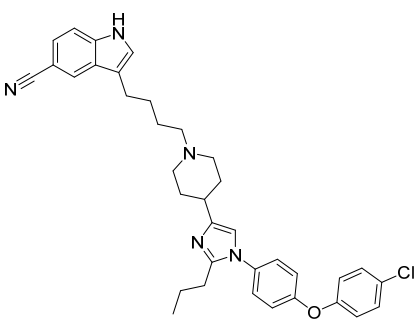
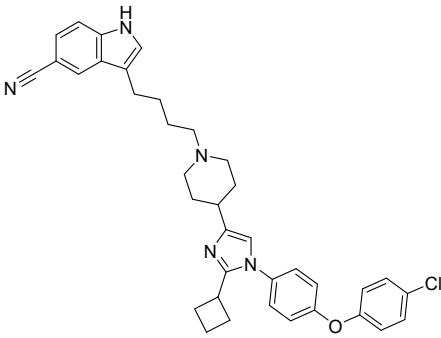
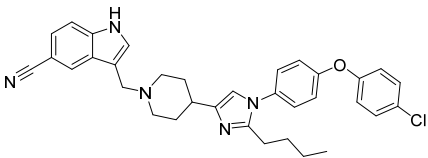
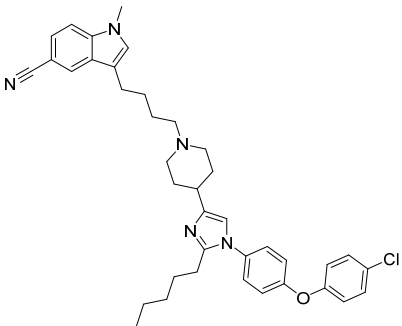
Compound	ChEMBL ID	Structure	RAGE IC ₅₀ [nM]	SERT IC ₅₀ [nM]
S10	CHEMBL5188606		12,920.0	65.58
S11	CHEMBL5192104		14,270	67.83
S12	CHEMBL5203206		8260	31.09
S13	CHEMBL5191418		3490	4.40
S14	CHEMBL5208902		12,490	7.77

Table 8. Cont.

Compound	ChEMBL ID	Structure	RAGE IC ₅₀ [nM]	SERT IC ₅₀ [nM]
S15	CHEMBL5175011		8290	7.47
S16	CHEMBL5194592		4040	57.73
S17	CHEMBL5180815		6030	15.05

Exploring different substituents on the thiazole core structure showed that, out of the alkyl substituents on thiazole, n-butyl was superior to methyl, ethyl, propyl, and isopropyl for RAGE inhibition, and out of the n-alkyl linkers between piperidine and indole, n = 4 was superior for dual inhibition.

Exploring different substituents on the imidazole core structure showed that, of the alkyl substituents on imidazole, ethyl, propyl, n-butyl, and cyclobutyl were superior to n-pentyl, isopropyl, cyclopropyl, cyclopentyl, cyclohexyl for RAGE inhibition, and out of the n-alkyl linkers between piperidine and indole, n = 1 and n = 4 were superior to n = 2 and n = 3 for dual inhibition.

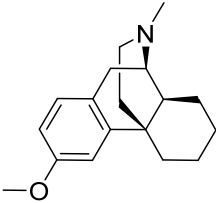
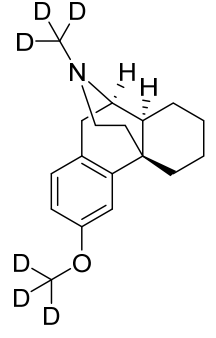
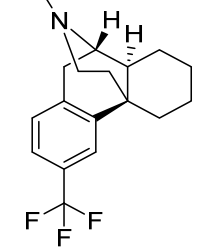
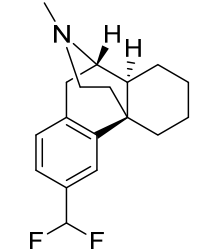
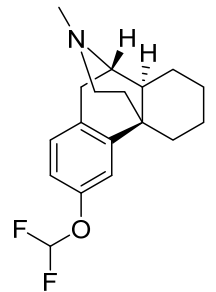
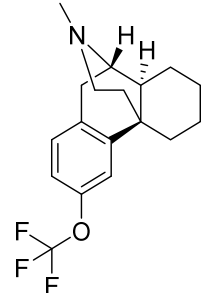
Out of the n-substituents on indole, H or methyl was most suitable, as increasing the size of the substituent decreased the dual inhibition.

Molecular-docking simulations to RAGE and SERT showed that **S12's** calculated pose was almost consistent with the calculated poses of the reference compounds (azeliragon and vilazodone) in their respective targets, with somewhat retained interactions, thus endorsing its biological activity. Furthermore, it had a better neuroprotective effect against β -amyloid_{25–35} than azeliragon and substantially lowered the immobility time in the tail suspension test, which indicates a potential antidepressant effect, yet was less potent than vilazodone. Although **S12** is the most promising molecule highlighted by the authors, it has not been returned by 6AWO-based pharmacophore screening.

In summary, **S12**, which is a first-generation dual RAGE/SERT inhibitor, has demonstrated the viability of the pharmacophore fusion strategy and offered a useful prototype for the possible treatment of AD with comorbid depression [49].

The next four novel compounds with the highest PhaseScreenScore, which emerged from the 6AWO-based pharmacophore screening, were **S2–S5**, along with dextromethorphan, which was the baseline structure of the novel compounds (Table 9) [48].

Table 9. Notable compounds explored in the fluoroalkylation of dextromethorphan study [48].

Compound	ChEMBL ID	Structure	$\sigma_1 K_i$ ¹ [nM]	$\sigma_2 K_i$ [nM]	NMDA K_i [nM]	SERT IC_{50} [nM]
Dextromethorphan	CHEMBL206132		73	862	624	56.0
AVP-786	CHEMBL5078675		n.t. ²	n.t.	n.t.	n.t.
S2	CHEMBL5086545		813	885	>10,000	60.0
S3	CHEMBL5081803		145	353	>10,000	24.0
S4	CHEMBL5093316		568	1281	>10,000	55.0
S5	CHEMBL5078388		757	833	>10,000	31.0

¹ Inhibition constant (K_i). ² Not tested (n.t.).

Dextromethorphan is a commonly used medicine, mainly as a cough suppressant, co-administrated with quinidine for the treatment of pseudobulbar affect and recently co-administered with bupropion for the treatment of major depressive disorder [53].

Dextromethorphan, like other aryl-methyl ethers, is subjected to in vivo O-dealkylation, yielding dextrorphan, which through N-methyl-d-aspartic acid receptor (NMDAR) inhibition may cause dissociative hallucinations when consumed in an excessive amount. As it facilitates dextromethorphan recreational use, efforts have been made to formulate a dextromethorphan analogue that is unusable for recreational use while still retaining the desirable pharmacological action [48]. Since dextromethorphan (co-administrated with bupropion) is indicated in the treatment of major depressive disorder and was also found (co-administrated with quinidine) to benefit levodopa-induced dyskinesia in PD, thus exhibiting valuable performance in treating other neurological and psychiatric diseases, it might be beneficial to explore its analogues [54,55]. This is further supported by the fact that AVP-786, its deuterated analogue, was studied in clinical trials (co-administrated with quinidine) for CNS disorders as well.

Common strategies to prevent O-dealkylation include fluorination and deuteration. Dextromethorphan may be fluorinated by replacing the aryl methyl ether with various fluoroalkyl ethers or fluoroalkyls. Overall, fluorinated dextromethorphan analogues sustained dextromethorphan's pharmacological profile, while having slightly weaker affinity to the σ_1 receptor (σ_1R), sustaining affinity to the σ_2 (σ_2R) receptor and ceasing affinity to NMDAR. Surprisingly, **S3** gained an affinity for sodium-dependent noradrenaline transporter (NET) ($IC_{50} = 944$ nM). Additionally, **S2–S5** also gained an affinity for SERT. Fluorinated analogues also maintained similar pharmacochemical properties compared to dextromethorphan, namely high aqueous solubility, while simultaneously improving the in vivo pharmacokinetics [48]. In comparison, deuteration did not show an influence on the pharmacokinetics and other drug-like properties compared to dextromethorphan. The selectivity and affinity to receptors exhibiting neuropsychiatric effects seem to also be unchanged, aside from blocking metabolism to dextrorphan, which blocks the ability to antagonize NMDAR [56]. Overall, fluoroalkylated and deuterated dextromethorphan analogues seem to be promising future therapeutic options for the treatment of CNS disorders, especially Parkinson-like disorders [48,57].

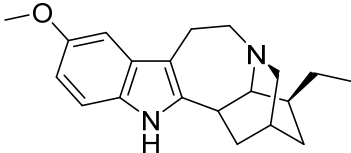
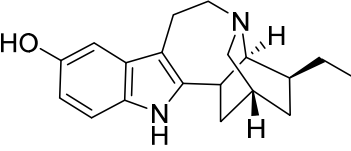
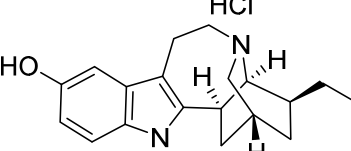
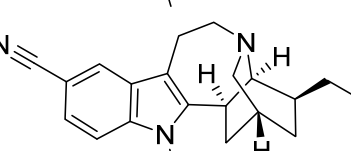
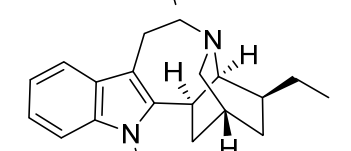
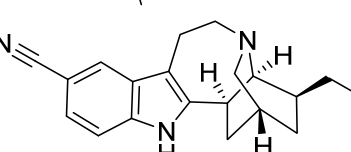
The last four compounds in the screening results were described in the 2022 patent for ibogaine and its analogues as therapeutics for neurological and psychiatric disorders, and the compositions and methods for treating psychiatric disorders or their symptoms were considered (Table 10) [51].

Ibogaine is an indole alkaloid, naturally occurring in *Tabernanthe iboga*, a shrub native to Central–West Africa. It is an unusual psychedelic substance that can cause vivid memory recall and replay as well as oneirogenic effects, which are states akin to waking dreams. While high doses of ibogaine are used for their hallucinogenic effects during religious rituals and initiation rites, low doses are used as stimulants to prevent fatigue on hunting excursions and to dull hunger and thirst. Ibogaine is effective in interrupting drug dependence by providing quick and long-lasting relief from cravings and withdrawal symptoms in anecdotal reports and open-label case studies involving individuals addicted to heroin and cocaine. First-pass metabolism quickly demethylates ibogaine into the long-acting metabolite noribogaine [51,58]. Ibogaine and noribogaine bind with modest affinity to a variety of targets, including transporters, SERT, NET, sodium-dependent dopamine transporter (DAT), and receptors, opioid, acetylcholine (ACh), σ and NMDA [59]. Based on the ibogaine analogues, which were the results of the screening, switching methoxy slightly increases the inhibition of vesicular monoamine transporter 2 (VMAT2), and greatly SERT. Phenyl analogues exhibit greater inhibition of VMAT2 and SERT. N-methylation of pyrrole also potentiates the inhibition of both VMAT2 and SERT.

Summarizing the above-mentioned studies, it can be concluded that compounds containing a 3-(4-(4-(1-(4-(4-chlorophenoxy)phenyl)-1H-imidazol-4-yl)piperidin-1-yl)butyl)-1H-indole-5-carbonitrile backbone or one in which the imidazole site is occupied by a

thiazole showed good SERT inhibitory activity (and some RAGE inhibitory activity on top). For SERT inhibition, the presence of an alkyl-substituted imidazole is most favorable (in particular, the ethyl and cyclobutyl substituents). Dextromethorphan derivatives with alkyl or alkoxyfluoro substituents have also achieved good activities against SERT. The noribogaine backbone gains SERT inhibitory activity upon N-methylation of the pyrrole and the conversion of the -OH group to a cyanide substituent.

Table 10. Notable compounds described in the patent for ibogaine and its analogues [51].

Compound	ChEMBL ID	Structure	VMAT2 IC ₅₀ [nM]	SERT IC ₅₀ [nM]
Ibogaine	CHEMBL1215855		4000.0	500.0 [51]
Noribogaine	CHEMBL5202868		570.0	280.0 [51]
S6	CHEMBL5207764		170.0	59.0 [51]
S7	CHEMBL5188930		440.0	5.1 [51]
S8	CHEMBL5201219		1500.0	80.0 [51]
S9	CHEMBL5175119		3300.0	26.0 [51]

3.2. Receptors

3.2.1. Dopamine Receptors

Dopamine is a catecholamine neurotransmitter that fulfills essential functions in both the CNS and PNS and is responsible for numerous effects: the inhibition of prolactin production, movement, behavior, motivation, the reward system, cognitive abilities including learning, attention, working memory, mood and even sleep. Dopamine acts via five dopamine receptors (D₁, D₂, D₃, D₄, and D₅) belonging to the G-protein-coupled receptors (GPCRs). Among them, two subclasses can be identified: the dopamine D₁-like family, which includes D₁ and D₅ receptors, and the D₂-like family, with D₂, D₃, and D₄ receptors. Types 2, 3, and 4 share only a similar chemical structure, while types 1 and 5 also have similar drug sensitivity. The D₁-like group are mostly postsynaptic receptors, binding mainly to the stimulatory G_s protein, while the D₂-like receptors are involved as

both postsynaptic receptors and presynaptic autoreceptors that bind to the inhibitory $G_{i/o}$ protein [60,61].

Dopamine D₁-like Family Receptors

D₁-like receptors are found primarily in the cerebral cortex, the striatum, and the limbic system of the brain. In addition, they are also present in the cardiovascular system, as well as taking part in the regulation of neuronal growth. D₁-like receptors are the most widespread of all the dopamine receptors in the human nervous system. D₁-like receptors also show an impact on behavior, with roles including impulse control and involuntary movements, sleep, effects on learning and working memory, the reward system, and even the growth regulation and renin control in the kidneys [60].

When dopamine binds to D₁-like receptors, guanosine nucleoside-binding proteins are activated, adenylyl cyclase activity is stimulated and, as a result, a cyclic AMP (cAMP) molecule is generated, acting as a secondary messenger. Other signaling pathways affect phospholipase C and calcium ion release. In the kidney and striatum, D₁-like receptors through the protein kinase A and C signaling pathways also affect adenosine 5'-triphosphatase (ATPase) inhibition [60].

Dopamine D₂-like Family Receptors

D₂-like receptors are expressed in high concentrations in the olfactory bulb, substantia nigra, ventral tegmental area (VTA), putamen, caudate and nucleus accumbens. In small concentrations, they can be also found in the circulatory system, kidneys, gastrointestinal tract, cerebral cortex, hypothalamus, sympathetic ganglia, septum, and adrenal glands. Unlike D₁-like receptors, D₂-like receptors inhibit the activity of adenylate cyclase and cause a decrease in the cAMP concentration [60].

Most dopamine receptor agonists approved for therapy are D₂-like receptors agonists (Table 11) [62,63]. These can be divided into ergoline, bromocriptine, and pergolide (withdrawn from human use by the FDA [64], it has some affinity for D₁R), and non-ergoline derivatives: pramipexole, ropinirole, and rotigotine. Apomorphine is a less specific agonist and acts on all the dopamine receptors, although mainly on D₂-like receptors [65].

Table 11. D₂-like receptor agonists indexed in ChEMBL.

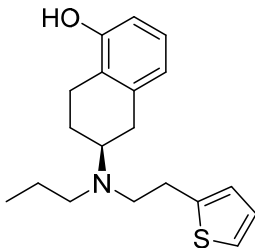
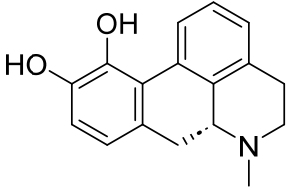
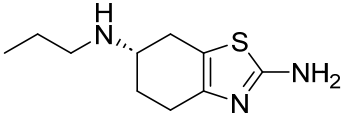
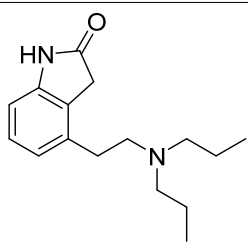
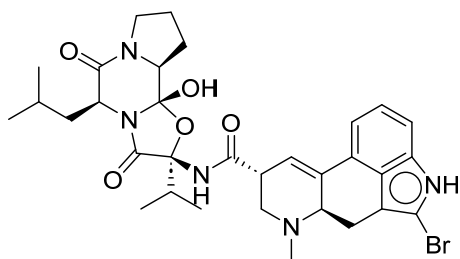
Compound	Structure	D ₂ R EC ₅₀ ¹ [nM]
Rotigotine		121.6
Apomorphine		1542.7
Pramipexole		14000.1

Table 11. Cont.

Compound	Structure	D ₂ R EC ₅₀ ¹ [nM]
Ropinirole		7999.4
Bromocriptine		27.8

¹ Half maximal effective concentration (EC₅₀).

Out of the structure of D₂R complexed with rotigotine (agonist; PDB ID: 8IRS), a pharmacophore model was proposed (Figures 6 and 7, Table 12).

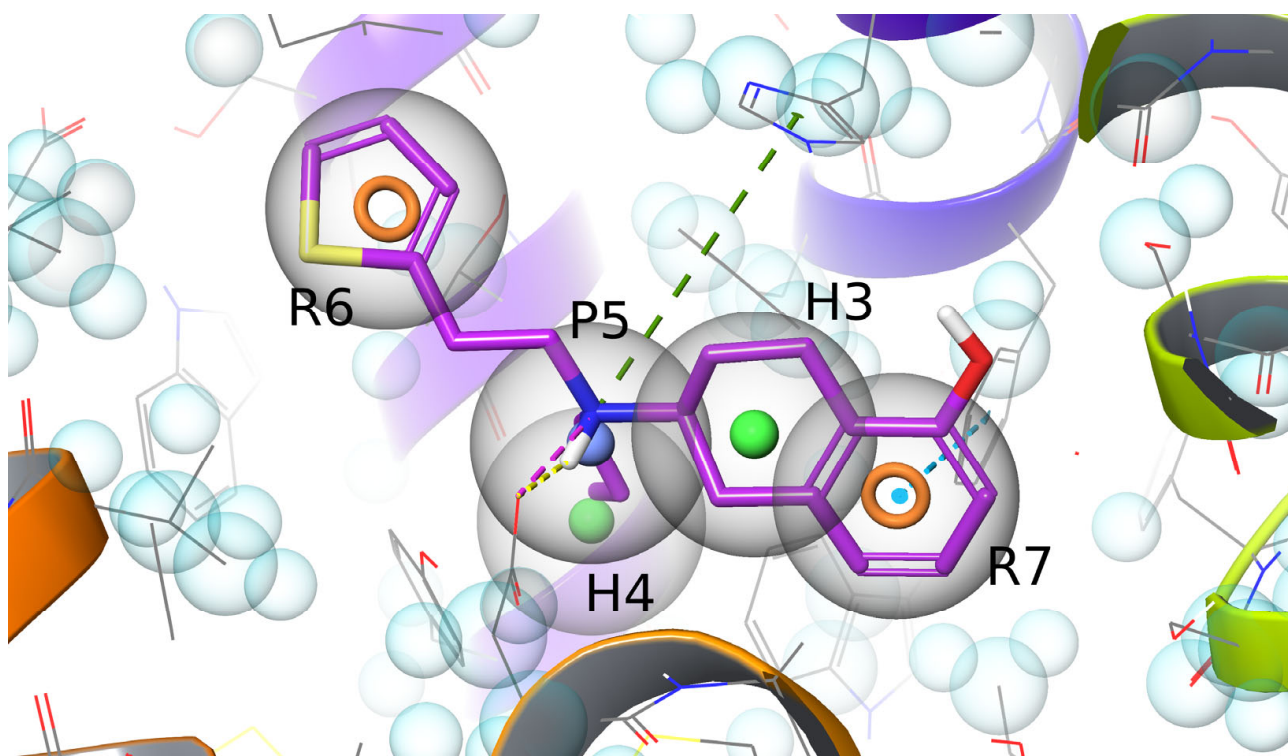


Figure 6. Rotigotine (purple) complexed with D₂R (gray) with, superimposed, the proposed pharmacophore model (balls and toruses). Dashed lines denote hydrogen bond (yellow), salt bridge (red), π - π stacking (blue), and π -cation interaction (green). Balls denote positive ionic feature (P, blue) and hydrophobic features (H, green), and toruses denote aromatic features (R, orange). Blue spheres denote excluded volumes.

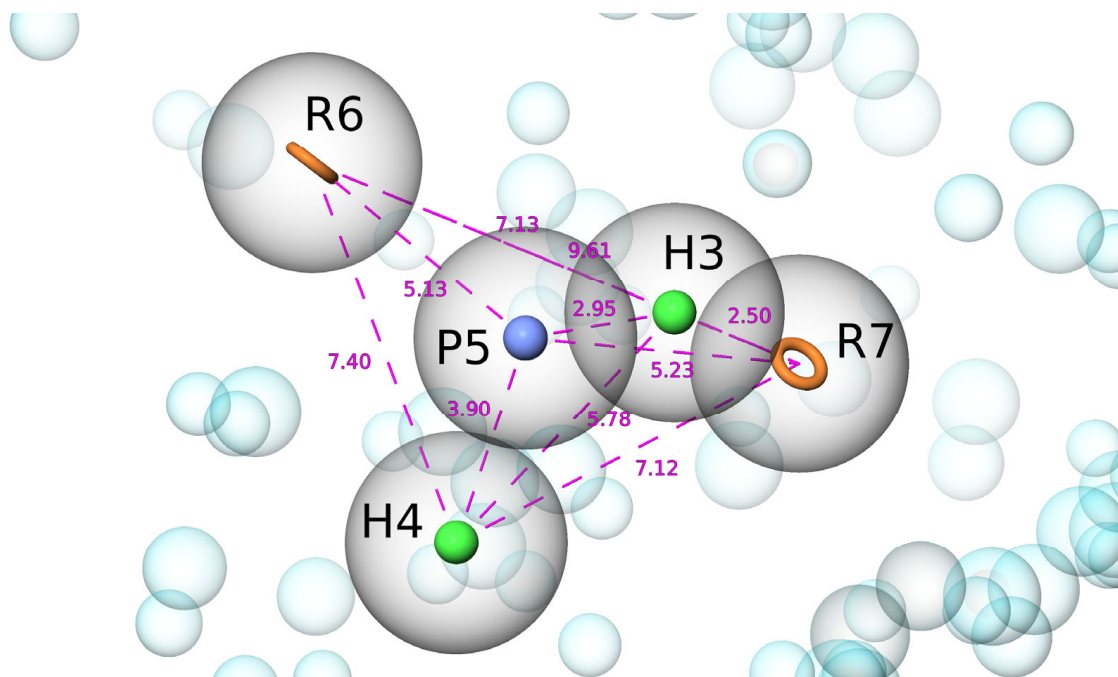


Figure 7. Proposed D₂R pharmacophore model derived from the 8IRS structure (balls and toruses). Balls denote positive ionic feature (P, blue) and hydrophobic features (H, green), and toruses denote aromatic features (R, orange). Dashed purple lines denote distances between features, with measurements in Å written beside them. Blue spheres denote excluded volumes.

Table 12. Distances (in Å) between the proposed D₂R pharmacophore model features.

Pharmacophore Features	H3	H4	P5	R6	R7
R7	2.50	7.12	5.23	9.61	
R6	7.13	7.40	5.13		
P5	2.95	3.90			
H4	5.78				
H3					

3.2.2. 8IRS (Dopamine D₂ Receptor) Pharmacophore Screening

In the ChEMBL database, we queried for molecules exhibiting a half maximal effective concentration (EC₅₀) ≤ 100 nM of human D₂-like receptor activation in assays published in 2020 and later, then conducted pharmacophore-based ligand screening using the model proposed by the Phase module (Table 13).

Table 13. D₂R pharmacophore screening results, including up to 10 hit molecules, excluding well-established medicines and pharmacological tools.

Compound	ChEMBL ID	Structure	PhaseScreenScore	D ₂ R EC ₅₀ [nM]
Propylnor-apomorphine	CHEMBL225230		2.148715	1.175 [66]
Quinpirole	CHEMBL240773		2.135124	1.18 [67]

Table 13. Cont.

Compound	ChEMBL ID	Structure	PhaseScreenScore	D ₂ R EC ₅₀ [nM]
Pramipexole	CHEMBL301265		2.102299	6.457 [68]
P1 (5-OH-DPAT)	CHEMBL273273		2.080779	41.0 [69]
P2	CHEMBL4781480		2.032088	3.4 [70]
P3	CHEMBL4470553		2.016313	7.7 [66]
P4	CHEMBL5267221		1.990749	13.4 [69]
P5	CHEMBL4555547		1.916507	0.373 [66]
P6	CHEMBL458088		1.819042	9.98 [71]
P7	CHEMBL5266134		1.801997	34.37 [69]
P8	CHEMBL4846101		1.798176	53.5 [67]
P9	CHEMBL4875081		1.765344	3.41 [67]
P10	CHEMBL4846472		1.765344	2.63 [67]

Three of the ten compounds resulting from our screening (**P1**, **P4**, and **P7**) appeared in a paper on bivalent dopamine agonists with cooperative binding and functional activity at D₂R, with modulating effects on alpha-synuclein protein aggregation and toxicity. The structures studied were a hybrid of pramipexole and **P1**, linked by various linkers [69]. In preceding studies, an increase in potency was achieved with the optimal length of the methylene linker of 7–10 methylene units [72]. In this study, the linker was modified by inserting more rigid moieties and introducing functional groups on the aromatic moiety of the linker [69]. One of the phenyl moieties was replaced by a bioisosteric 2-aminothiazole moiety (**P4**) and affinity to both dopamine D₂R and D₃ receptor (D₃R) was maintained (D₂R IC₅₀ = 13.4 nM, D₃R IC₅₀ = 13.3 nM). This compound appeared in seventh place in our screening, and in the described study [69], it turned out to be the most active structure. It was also one of the few compounds that aligned with all the pharmacophoric properties of the Phase pharmacophore model. The addition of hydroxyl groups at positions 1 and 4 to the aromatic linker ring in the presence of two isosteric 2-aminotiazole rings in the **P7** slightly reduced the affinity for D₂R yet was still higher than for the reference molecule **P1** (IC₅₀ = 34.37 nM vs. 41.0 nM). The hydroxyl groups themselves were well tolerated, while the presence of a thiazole-2-amino group in **P4** and **P7** had a moderate effect on the reduction of D₂R potency. **P1** and **P7** met four out of five features of our pharmacophore model, both lacking one aromatic trait [69].

DPAT's structure was also explored in another study [71], in which its 7-hydroxy derivative was modified by the addition of *n*-phenylpiperazine to the alkyl chain by a heterocyclic nitrogen atom, yielding **P6**, a potent D₂R (EC₅₀ = 9.98 nM) and D₃R (EC₅₀ = 2.91 nM) dual agonist. Further SAR studies discovered that the 2-(piperazin-1-yl)ethan-1-amine backbone is crucial for excellent dual activity. Bulky substituents (biphenyl or indole) at the piperazine N atom exhibit potent D₃R activity, especially 2,3-dichlorophenyl. Propyl substitution at the alkyl amine increases the activity. 6-(5,6,7,8-tetrahydronaphthalen-1-ol)yl is more favorable for 6-(4,5,6,7-tetrahydrobenzo[d]thiazol-2-amine)yl, as well as an R to S configuration, for D₃R binding. Overall, the most potent molecule (D₂R EC₅₀ = 0.87 nM, D₃R EC₅₀ = 0.23 nM) appeared to be (S)-6-((2-(4-(9H-carbazol-2-yl)piperazin-1-yl)ethyl)(propyl) amino)-5,6,7,8-tetrahydronaphthalen-1-ol, which is 2-(piperazin-1-yl)ethan-1-amine with 2-(9H-carbazol)yl substitution at the piperazine N atom and propyl and 6-(5,6,7,8-tetrahydronaphthalen-1-ol)yl substitution at the ethanamine atom [71].

One of the compounds (**P2**, propyl aminoindane), turned out to be a well-known compound that is an alkylated D₂R agonist. It appeared in the study [70] as a molecule that, after appropriate modification (a biphenyl and an alline handle were attached to one of the N-propyl substituents of the aminoindane), served as a compound for the synthesis of two series of bidentate ligands selectively targeting D₂R heterodimers.

P3 and **P5** emerged from the study of the structure–functional–selectivity relationship of novel apomorphine analogues to develop selective D₁R and D₂R dual agonists, functionally biased toward activating the arrestin signaling pathway [66]. Overactivation of the G-protein pathway is associated with dyskinesias, while recruitment of β-arrestin 2 may not only desensitize the G-protein pathway but additionally activate the G-protein independent pathway, which can alleviate locomotor symptoms. Furthermore, both D₁R and D₂R activation are needed for a potent locomotor response. Compared to apomorphine, which is nonselective toward D₁R (IC₅₀ = 3.77 nM) and D₂R (IC₅₀ = 1.61 nM), propylnorapomorphine exhibits stronger affinity to D₁R (IC₅₀ = 1.1 nM) and D₂R (IC₅₀ = 0.04 nM), owing to elongation of the N-alkyl chain. O-acetylation of the catechol group of propylnorapomorphine yielded **P5**, which exhibits lesser affinity to D₁R (IC₅₀ = 31.7 nM) and maintains affinity to D₂R (IC₅₀ = 0.373 nM). Methylendioxy protection of the catechol group of propylnorapomorphine yielded **P3**, which has an affinity to D₁R (IC₅₀ = 717.5 nM) and slightly lower to D₂R (IC₅₀ = 7.7 nM) compared to propylnorapomorphine. In the case of β-arrestin recruitment, apomorphine is biased toward recruitment for D₂R (IC₅₀ = 10.1 nM) rather than D₁R (IC₅₀ = 520.8 nM). In propylnorapomorphine, elongation of the N-alkyl chain further deepens this bias for D₂R (IC₅₀ = 1.18 nM) compared to D₁R (IC₅₀ = 1884 nM).

O-acetylation of the catechol group in the case of **P5** slightly diminished recruitment for D₂R (IC₅₀ = 6.34 nM), while greatly lowering for D₁R (IC₅₀ = 5496 nM). Lastly, methylenedioxy protection of the catechol group of **P3** resulted in the inhibition of β -arrestin recruitment, both for D₂R (IC₅₀ = 520 nM) and for D₁R (IC₅₀ = 1949 nM) [66].

P8–P10 [67] were described in a paper that investigated 2-phenylcyclopropylmethylamine (PCPMA) derivatives for partial agonism at the D₂R. The **P8** compound was formed by the propylation of the secondary amino group in the PCPMA part. This did not result in an improvement in its activity (EC₅₀ = 53.5 nM). **P10** with a chlorine atom on the phenyl ring in the para position relative to the methoxy substituent showed an increase in activity, had the best activity toward the D₂R among all the new compounds in the entire study (EC₅₀ = 2.63 nM), and, in our screening, had the highest activity [67].

Paying attention to the results, it seems that, for activity against D₂R, the (S)-N6-(2,5-dimethyl-4-(2-(propylamino)ethyl)phenethyl)-N6-propyl-4,5,6,7-tetrahydrobenzo[d]thiazole-2,6-diamine backbone linked to a hydroxynaphthalene substituent via a second amine group might be a promising scaffold. Compounds that are modifications of propylapomorphine also showed good activity—beneficial here seems to be the O-acetylation of the catechol group, on the other hand. Moreover, 2-phenylcyclopropylmethylamine derivatives containing an (S)-N6-(2,5-dimethyl-4-(2-(propylamino)ethyl)phenethyl)-N6-propyl-4,5,6,7-tetrahydrobenzo[d]thiazole-2,6-diamine substituent also constitute a promising area for exploration. Here, the presence of a chlorine atom on the phenyl ring at the para position relative to the methoxy substituent proved most favorable for SAR. For dual D₂R and D₃R activity, structures based on an N-(2-(piperazin-1-yl)ethyl)propan-1-amine core, with bulky, hydrophobic substitutions at the heterocyclic N atom and 6-(5,6,7,8-tetrahydronaphthalen-1-ol)yl substitution at the alkyl N atom with R configuration, might find use as template structures.

3.2.3. Serotonin Receptors

Serotonin receptors are divided into seven receptor families: 5-HT₁, 5-HT₂, 5-HT₃, 5-HT₄, 5-HT₅, 5-HT₆, and 5-HT₇. In total, at least 14 subtypes of these receptors have been discovered. All the families except 5-HT₃Rs belong to the GPCRs. In turn, 5-HT₃Rs are sodium–potassium ligand-gated ion channels [73].

The 5-HT₁Rs and 5-HT₅Rs are coupled to the G_i/G_o protein; their activation causes a decrease in the intracellular cAMP concentration. 5-HT₂Rs are coupled to the G_{q11} protein, and their activation causes an increase in the inositol trisphosphate (IP₃) and diacylglycerol (DAG) concentrations. 5-HT₄Rs, 5-HT₆Rs, and 5-HT₇Rs are coupled to the G_s protein; therefore, when activated, the cellular cAMP concentrations increase. All the receptor families are found in the CNS, where they are responsible for mood, learning, memory, sleep, locomotion, addiction, feelings of anxiety, or thermoregulation, among other things. Some are also found in the vascular system (5-HT₁Rs, 5-HT₂Rs, 5-HT₇Rs) and gastrointestinal tract (5-HT₂Rs, 5-HT₃Rs, 5-HT₄Rs), while 5-HT₂Rs are also found in platelets and smooth muscle, and 5-HT₃Rs are also found in the PNS [74].

5-HT_{1A} Receptor

The 5-HT_{1A}R is one of the best-studied serotonin receptors as the main serotonin inhibitory receptor in the brain. Two populations of this receptor can be distinguished—auto- and heteroreceptors. As an autoreceptor, it appears at presynaptic terminals in the sutural nuclei, where it controls the excitation of serotonergic neurons and the secretion of neurotransmitters. Heteroreceptors are expressed on non-serotonergic neurons, appearing mainly in the limbic system (body and dendrites of glutamatergic neurons, axons of γ -aminobutyric acid (GABA) neurons, or cholinergic neurons). Some receptors regulate the release of ACh (medial septum), glutamate (prefrontal cortex), or dopamine (midbrain cap) [73,75].

Because of its importance in the pathophysiology of neuropsychiatric disorders such as depression and anxiety [76], we chose it as a target for pharmacophore-based screening.

Out of the structure of 5-HT_{1A}R complexed with serotonin (agonist; PDB ID: 7E2Y), a pharmacophore model was proposed (Figures 8 and 9, Table 14).

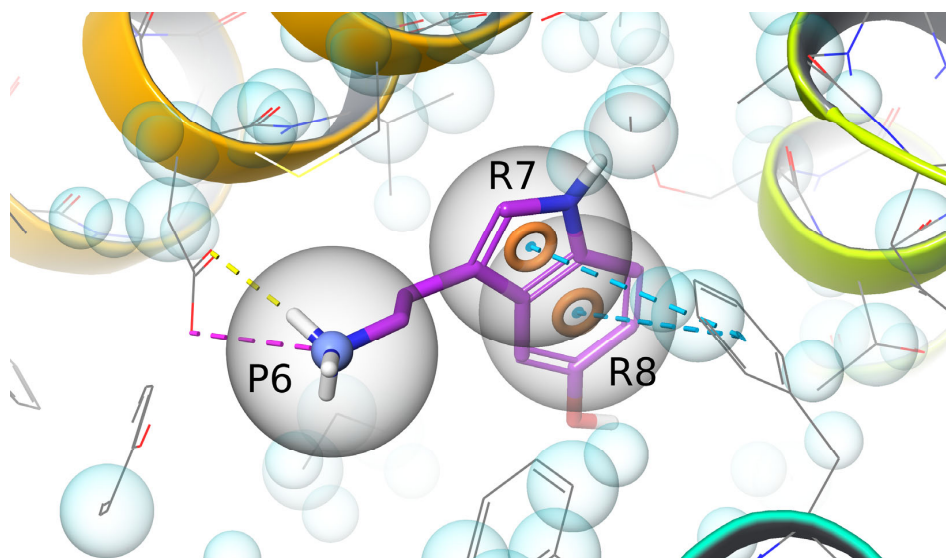


Figure 8. Serotonin (purple) complexed with 5-HT_{1A}R (gray) with, superimposed, the proposed pharmacophore model (ball and toruses). Dashed lines denote hydrogen bond (yellow), salt bridge (red) and π - π stacking interactions (blue). Ball denotes positive ionic feature (P, blue) and toruses denote aromatic features (R, orange). Blue spheres denote excluded volumes.

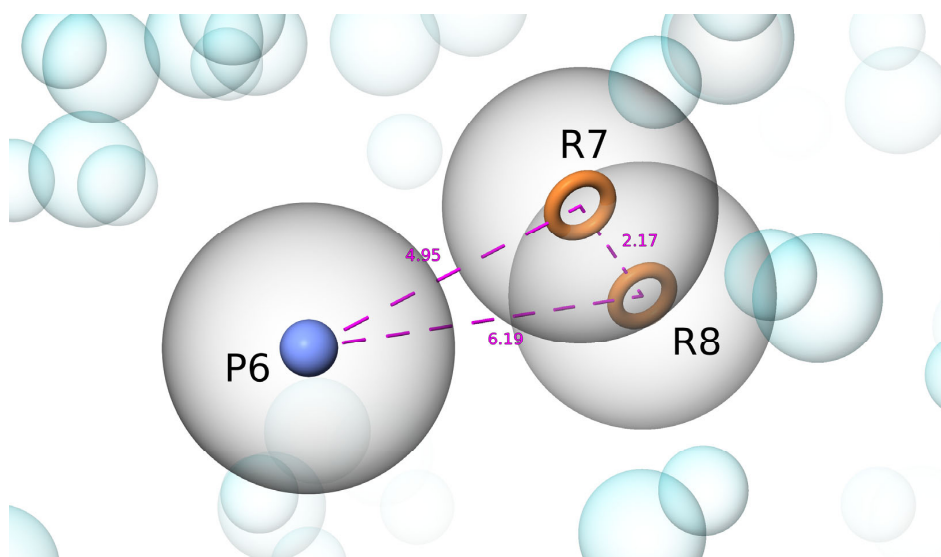


Figure 9. Proposed 5-HT_{1A}R pharmacophore model derived from the 7E2Y structure (ball and toruses). Ball denotes positive ionic feature (P, blue) and toruses denote aromatic features (R, orange). Purple dashed lines denote distances between features, with measurements in Å written beside them. Blue spheres denote excluded volumes.

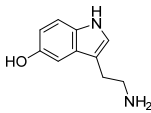
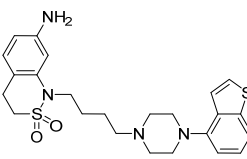
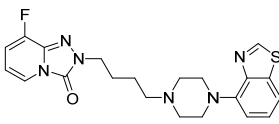
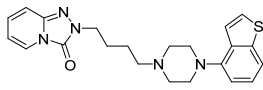
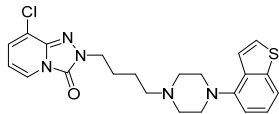
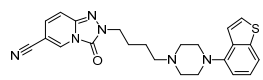
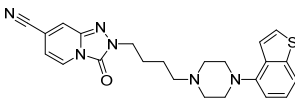
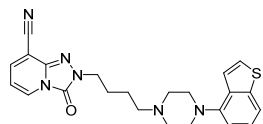
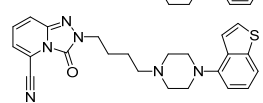
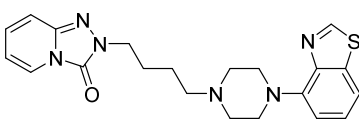
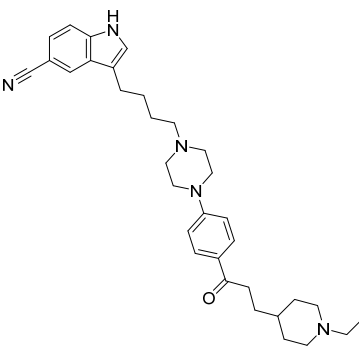
Table 14. Distances (in Å) between the proposed 5-HT_{1A}R pharmacophore model features.

Pharmacophore Features	P6	R7	R8
R8	6.19	2.17	
R7	4.95		
P6			

3.2.4. 7E2Y (Serotonin 5-HT_{1A} Receptor) Pharmacophore Screening

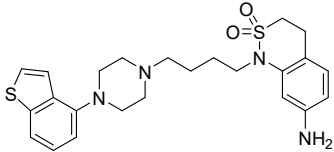
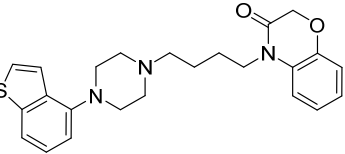
From the ChEMBL database, we queried for molecules exhibiting an EC₅₀ ≤ 100 nM of human 5-HT_{1A}R activation in assays published in 2020 and later, then conducted pharmacophore-based ligand screening using the model proposed by the Phase module (Table 15).

Table 15. 5-HT_{1A}R pharmacophore screening results, including up to 10 hit molecules, excluding well-established medicines and pharmacological tools.

Compound	ChEMBL ID	Structure	PhaseScreenScore	5-HT _{1A} EC ₅₀ [nM]
Serotonin	CHEMBL39		2.890	10.0 [77]
H1	CHEMBL4751542		2.103	0.7943 [78]
H2	CHEMBL4633397		2.030	0.1 [79]
H3	CHEMBL4638599		2.020	1.7 [79]
H4	CHEMBL4636321		2.010	12.1 [79]
H5	CHEMBL4644391		1.998	9.7 [79]
H6	CHEMBL4648979		1.998	5.9 [79]
H7	CHEMBL4638430		1.997	1.4 [79]
H8	CHEMBL4644742		1.997	20.2 [79]
H9	CHEMBL4635890		1.874	2.8 [79]
H10	CHEMBL5079986		1.790	9.0 [50]

The highest score value was calculated for **H1**, developed in the study exploring multi-target 5-HT_{1A}R agonists and D₂R, 5-HT_{2A} receptor (5-HT_{2A}R) antagonists as schizophrenia drug candidates by automated deep-learning workflow. Typical antipsychotics are mainly D₂R antagonists and exhibit good control of positive schizophrenia symptoms but cause various side effects like Parkinson-like extrapyramidal symptoms or tardive dyskinesia. Atypical antipsychotics usually exhibit inhibition (low affinity) toward D₂R and (high affinity) 5-HT_{2A}R, which facilitates less risk of side effects, but exhibit unsatisfactory control of cognitive dysfunction and negative symptoms. 5-HT_{1A}R agonism may improve control of cognitive dysfunction and negative symptoms and alleviate side effects. The currently used atypical antipsychotics have a low ratio of 5HT_{1A}R/D₂R affinity and the higher ratio may improve the aforementioned pharmacodynamics of antipsychotics. The goal was to find novel structures, exhibiting high activity and low similarity, using deep-learning model assembly. To do so, two deep neural networks were built and then trained on data from the GLASS, Reaxys, and SciFinder databases. Out of the identified molecules, **H11** exhibited the strongest affinity toward 5-HT_{1A}R. Its derivatization yielded **H1**, which exhibited the second-best 5-HT_{1A}R affinity and emerged in pharmacophore screening (Table 16). It was noticed that similar compounds with a two-atom linker length had lower activities in relation to all three targets than compounds with a four-atom linker length. Fluorinated compounds displayed stronger agonism to 5-HT_{1A}R [78].

Table 16. Two most potent 5-HT_{1A}R agonists from a multitarget schizophrenia drug study [78].

Compound	ChEMBL ID	Structure	D ₂ IC ₅₀ [nM]	5-HT _{2A} IC ₅₀ [nM]	5-HT _{1A} EC ₅₀ [nM]
H1	CHEMBL4751542		67.61	2.818	0.7943
H11	CHEMBL4741908		216.0	1.64	0.51

Eight of the ten results of our screening (**H2–H9**) were described in one study [79], in which a new class of antipsychotic drugs was synthesized with a triazolopyridinone system linked to substituted piperazine or piperidine. The compounds obtained showed activity against 5-HT_{1A}R (agonism), as well as 5-HT_{2A}R and D₂R (antagonism). The SAR for both serotonin and dopamine receptors was related to the variation of substituents on the triazolopyridinone ring and piperidine groups. **H3** with a triazolopyridinone scaffold showed good agonist activity on 5-HT_{1A}R (EC₅₀ = 1.7 nM) and high antagonistic activity against 5-HT_{2A}R (IC₅₀ = 34.2 nM) and against D₂R (IC₅₀ = 12.4 nM). To obtain further compounds, different substituents were introduced into the [1,2,4]triazolo [4,3-a]pyridin-3(2H)-one ring at positions 5–8. The introduction of halogen substituents into the ring at positions 6 and 8 resulted in a decrease in activity toward D₂R and 5-HT_{2A}R, while the activity toward the 5-HT_{1A}R remained high, e.g., the **H4** captured by our screening expressed activity toward the 5-HT_{1A}R of EC₅₀ = 12.1 nM. Cyano and methoxy substituents were successively added to the above-mentioned ring at different positions as well. **H8** with the cyano substituent at position 5 was the least active against 5-HT_{1A}R among the results of our screening (EC₅₀ = 20.2 nM). On the other hand, **H6** with the cyano substituent at position 7 performed better in the biological tests (EC₅₀ = 5.9 nM). **H5** with a 6-cyano substitution and **H7** with an 8-cyano substitution of [1,2,4]triazolo [4,3-a]pyridin-3(2H)-one achieved very good D₂R inhibitory activity (IC₅₀ = 1.03 nM and 1.5 nM, respectively) while maintaining, especially **H7**, good agonist activity on 5-HT_{1A}R (EC₅₀ = 9.7 nM and

1.4 nM). These results suggest the influence of the substituent position for this group of compounds. In **H9**, the thiophene ring was exchanged for a thiazole ring, and in **H2**, a fluorine substituent additionally appeared at position 8 of the thiazolpyrrolidine. This led to a sharp decrease in activity against 5-HT_{2A}R and D₂R for **H9** (IC₅₀ = 117 nM and 2730 nM) while maintaining good activity against 5-HT_{1A}R (EC₅₀ = 2.8 nM). **H2** showed better activity at all three receptors and fantastic activity against the 5-HT_{1A}R (EC₅₀ = 0.1 nM).

The last hit described herein—**H10**—came from research focused on [50] the search for chimeric vilazodone-donepezil derivatives targeting 5-HT_{1A}R, SERT, and acetylcholinesterase (AChE) [50]. Such compounds were expected to be an ideal response to depression co-occurring with Alzheimer's disease. **H10** was the second most active against the 5-HT_{1A}R (EC₅₀ = 9.0 nM)—the introduction of vinyl instead of a methyl substituent at the 1-methylpiperidine moiety resulted in even higher potency (EC₅₀ = 8.6 nM). Under the assumptions of the aforementioned work, compounds showing good activity on all three targets, including SERT and AChE, were found to be superior overall to **H10**, even though on the 5-HT_{1A}R alone its activity was almost the best. Our model focused exclusively on 5-HT_{1A}R, so it can be said that it did well in this screening by typing just this compound [50].

Summarizing the above studies, for activity toward the 5-HT_{1A}R, as well as the dopamine D₂R, compounds built on a 2-(4-(4-(4-(benzo[d]thiazol-4-yl)piperazin-1-yl)butyl)-[1,2,4]triazolo [4,3-a]pyridin-3(2H)-one backbone or one in which the thiazole is replaced by a thiophene ring are beneficial. The most favorable according to the local SAR analysis is the presence of a fluorine or cyano group at position 8 of the [1,2,4]triazolo [4,3-a]pyridin-3(2H)-one scaffold. The position of the substituent plays an important role in SAR in these compounds. Furthermore, a similar backbone to the above-described one, containing the stannous 2,2-dioxide 7-amino-1-methyl-3,4-dihydro-1H-benzo[c][1,2]thiazine instead of the 2-methyl-[1,2,4]triazolo [4,3-a]pyridin-3(2H) one, also shows good activity against 5-HT_{1A}R and D₂R. This dual-target interaction might also be deduced from the proposed pharmacophore models derived for both D₂R and 5-HT_{1A}R—in both cases, a positively ionizable feature, an aromatic feature as well as a hydrophobic or aromatic feature could be visible, and the ligands described herein align with these features (given the similar hydrophobic properties of aromatic rings and hydrophobic moieties). Moreover, it might also overlap with the SERT and MAO-B ones (Figure 10)—modifications of the compound **H10** provided herein provided activity not only for 5-HT_{1A}R but also targets such as SERT and AChE.

3.3. Pharmacophore Model Alignment

Based on the publications described earlier, the search for multi-target ligands became an everyday practice. Of the targets we selected and for the studies described above, such combinations succeeded for the 5-HT_{1A}R and D₂R, and 5-HT_{1A}R and SERT, pairs—where the designed molecules showed good activity more than once.

We decided to overlay the generated proposed models using Phase's Hypothesis Alignment function to assess whether it would be possible to find molecules with multi-target activity on all, or at least most, of our chosen targets (Figure 10). Analyzing the pharmacophores, it can be seen that all four proposed pharmacophore models present common features: each contains a positively ionizable feature and at least one aromatic feature, and three of them also have a hydrophobic feature. When the models are overlaid, the positively ionizable features are in a fairly similar position, and the groups of aromatic and hydrophobic features also mostly overlap.

The similarity of the pharmacophore models derived from different target complexes suggests that it is fairly possible to obtain a multi-target structure, which could exhibit the desired activity on MAO-B, SERT, 5-HT_{1A}R, and D₂R, devoid of possible side effects, and potentially alleviate symptoms such as depression and motor dysfunctions. Based on the constructed models and their averaging, such a chemical structure would meet the characteristics of a pharmacophore for a D₂R-based model—having one positive ionic feature, two aromatic features, and one hydrophobic feature, with a possibility of variation

between the presence of additional hydrophobic or aromatic feature—with the distances between all the features roughly maintained (Figure 11).

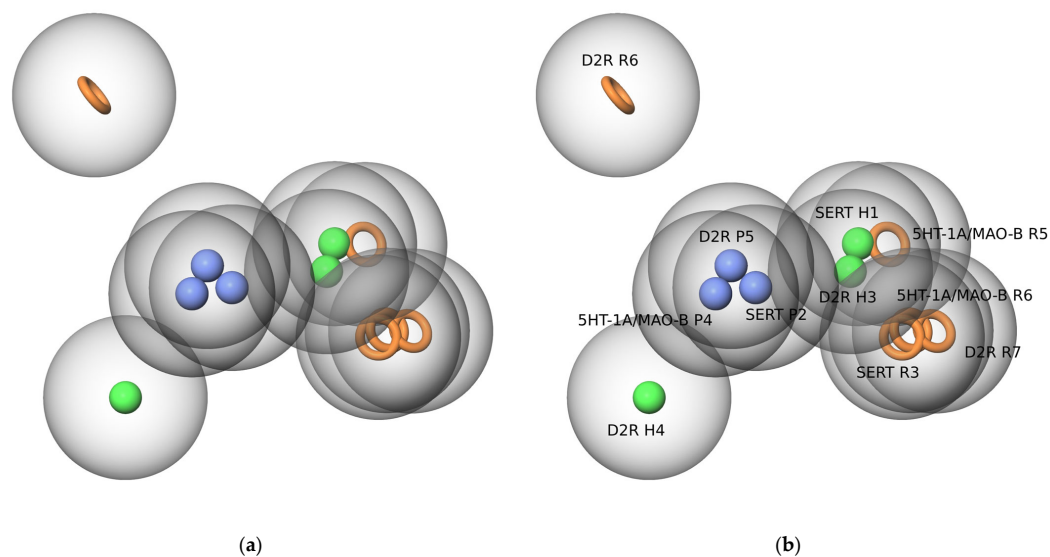


Figure 10. (a) Alignment of four proposed pharmacophore models (MAO-B, SERT, 5-HT_{1A}R, D₂R) used in this review (balls and toruses). (b) Balls denote positive ionic features (P, blue) and hydrophobic features (H, green), and toruses denote aromatic features (R, orange). The origin of each of the features has been described in capital letters.

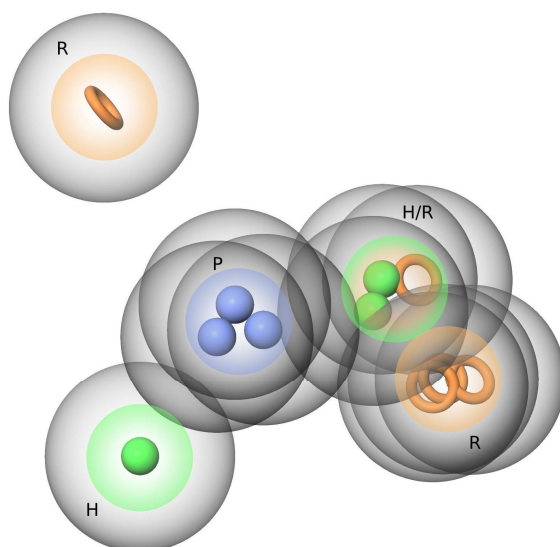


Figure 11. Averaged pharmacophore model based on the previously aligned models (balls and toruses). Balls denote positive ionic features (blue) and hydrophobic features (green), and toruses denote aromatic features (orange). Glowing spheres denote the averaged model's features: positive ionic feature (P, blue), hydrophobic feature (H, green), hydrophobic or aromatic feature (H/R, green-orange gradient) and aromatic features (R, orange).

4. Materials and Methods

A database search was conducted using the ChEMBL database [25]. The protein structures were obtained from the PDB, then prepared using the Maestro Schrödinger suite [80], using the Protein Preparation Wizard (default settings) [81,82]. The compounds' structures were prepared using LigPrep (default settings) [83]. The pharmacophore models were generated using Phase (default settings unless otherwise specified). The pharmacophore screening was conducted using Phase (default settings) [22,23,84].

5. Conclusions

PeD has an extraordinarily strong impact on the lives of patients, and to the best of our knowledge, there are no specific medications and recommendations focused on this disease. Due to the similarity of the symptoms, treatment consists of administering the same drugs that are used in PD and providing only symptomatic treatment. Therefore, we see a lot of room for further research here, both for symptomatic drugs, which we have considered in this review, and for biological drugs that could change the fate of patients.

Therefore, herein, we reviewed section by section novel, active compounds that might either serve as hits for further optimization or candidates for further phases of studies, leading to potential use in the treatment of PeD. Due to the complex nature of the symptoms, we focused on several major therapeutic targets—the MAO-B, and SERT enzymes, as well as the D₂R and the 5-HT_{1A}R. We were able to propose pharmacophore models for each of the targets, which helped us to select, in our opinion, the compounds best suited in terms of the chemical structure, whose backbones are the newest directions from which medicinal chemistry can be further explored.

We believe that further research focused on multi-target ligands would be the most comprehensive approach for further symptomatic PeD treatment. Based on the analysis performed within the described studies and our proposed pharmacophore models, including their alignment, it is apparent that this is possible and can yield promising results. Especially, molecules based on the averaged/D₂R model, which could exhibit an effect on all the studied targets—MAO-B, SERT, D₂R, and 5-HT_{1A}R—easing parkinsonism and depressive symptoms alike. In this context, the results of our comprehensive computer-aided analysis can be beneficial in finding such molecules, which proved safe and effective in preclinical and clinical studies, which would mean fewer drugs that a patient with PeD has to take at the same time, thus increasing the quality of the patient's life.

Designing compounds that are multi-targeted carries numerous potential risks. Such compounds may act not only on the desired biological targets but also on off-targets. Subtypes of the same receptor family, in most cases, share a high level of structural similarity; therefore, the pharmacophores of the molecules acting on them might also overlap. This might drastically affect the selectivity of the desired compound over the main target. For instance, two of the serotonin receptors, namely 5-HT_{2B} and 5-HT_{2C}, represent the best example of such. Due to the high dimensionality of the data, the complexity of the neurological pathways to tackle, numerous targets and off-targets to be considered, and similarities between pharmacophore models, the help of precise data analysis through artificial intelligence (AI) may prove useful in the further exploration of the increasingly expanding vast accessible chemical space [85,86].

While the significant challenges of finding drugs for rare diseases have already been described in Section 1.2, it is worth remembering that the search for any new drug to hit the market is a serious venture. Even if a substance will fit the proposed pharmacophore and would meet all of the hit/lead compound requirements, its journey from the laboratory bench to the patient's bedside is exceptionally long. Once we have found (through *in silico* models) a molecule that should work on the screen, the path of such a potential drug might seem unending, starting from *in vitro* biological affinity and ADME-Tox studies, and extensive testing of the molecule's physiochemical properties, with the next stop being *in vivo* models, primarily for toxicity. Only then, after being proven active and stable, do the three phases of clinical trials await, where the drug is evaluated for safety and efficacy first on healthy individuals, then on sick patients. At any stage of this long process, a drug candidate may not turn out to be good enough [87,88]. On top of this, clinical trials for rare genetic diseases face several additional challenges, such as difficulties in patient recruitment, gaps in basic research, ethical concerns, regulatory hurdles, or more down-to-earth matters such as economic profitability.

Thus arises the importance of translational research, especially in the search for orphan drugs. By assembling diverse multidisciplinary research teams, the process of translating basic research findings into novel therapies can be shortened. Additionally, bi-directional

knowledge circulation between researchers, and clinical and social personnel has been suggested to speed up these breakthroughs [14].

Additionally, we can see that research on rare diseases and common diseases is interlocked more than was thought, in such a way that they can both fuel each other's findings; e.g., research on better PD and depression medicines can improve PeD treatment and vice versa. Therefore, the search for the best possible therapy—in this case, for PeD—poses a particular challenge to complex research teams. In light of the use of increasingly sophisticated computational methods, a reality check, based on human knowledge, intuition, and communication, cannot be forgotten. Hence, the considerations described in our paper undoubtedly contribute to the development of these global and comprehensive efforts to improve PeD therapy.

Supplementary Materials: The following supporting information can be downloaded at <https://www.mdpi.com/article/10.3390/ijms251910652/s1>.

Author Contributions: Conceptualization, Z.G., M.H., J.H. and K.J.K.; methodology, Z.G., M.H. and K.J.K.; software, Z.G., M.H. and K.J.K.; validation, Z.G. and M.H.; formal analysis, Z.G. and M.H.; investigation, Z.G. and M.H.; resources, K.J.K.; data curation, Z.G. and M.H.; writing—original draft preparation, Z.G. and M.H.; writing—review and editing, Z.G., M.H., J.H. and K.J.K.; visualization, Z.G.; supervision, K.J.K.; project administration, J.H. and K.J.K.; funding acquisition, J.H. and K.J.K. All authors have read and agreed to the published version of the manuscript.

Funding: This research was partly funded by Jagiellonian University Projects no. N42/DBS/000331 and N42/DBS/000385.

Data Availability Statement: The original contributions presented in this study are included in the article and Supplementary Materials; further inquiries can be directed to the corresponding author.

Acknowledgments: We acknowledge the usage of Smart—Servier Medical Art (CC BY 4.0) in creating the figures (<https://smart.servier.com/> (accessed on 10 July 2024)). The DeepL translator (<https://www.deepl.com/en/translator> (accessed on 10 July 2024)) and ChatGPT (<https://openai.com/chatgpt/> (accessed on 10 July 2024)) services were used as text redaction tools.

Conflicts of Interest: The authors declare no conflicts of interest.

References

1. Wilson, D.M.; Cookson, M.R.; Van Den Bosch, L.; Zetterberg, H.; Holtzman, D.M.; Dewachter, I. Hallmarks of Neurodegenerative Diseases. *Cell* **2023**, *186*, 693–714. [CrossRef] [PubMed]
2. 2024 Alzheimer's Disease Facts and Figures. *Alzheimer's Dement.* **2024**, *20*, 3708–3821. [CrossRef] [PubMed]
3. Marras, C.; Beck, J.C.; Bower, J.H.; Roberts, E.; Ritz, B.; Ross, G.W.; Abbott, R.D.; Savica, R.; Van Den Eeden, S.K.; Willis, A.W.; et al. Prevalence of Parkinson's Disease across North America. *NPJ Park. Dis.* **2018**, *4*, 21. [CrossRef] [PubMed]
4. Dugger, B.N.; Dickson, D.W. Pathology of Neurodegenerative Diseases. *Cold Spring Harb. Perspect. Biol.* **2017**, *9*, a028035. [CrossRef]
5. Lamprey, R.N.L.; Chaulagain, B.; Trivedi, R.; Gothwal, A.; Layek, B.; Singh, J. A Review of the Common Neurodegenerative Disorders: Current Therapeutic Approaches and the Potential Role of Nanotherapeutics. *Int. J. Mol. Sci.* **2022**, *23*, 1851. [CrossRef]
6. Nguengang Wakap, S.; Lambert, D.M.; Olry, A.; Rodwell, C.; Gueydan, C.; Lanneau, V.; Murphy, D.; Le Cam, Y.; Rath, A. Estimating Cumulative Point Prevalence of Rare Diseases: Analysis of the Orphanet Database. *Eur. J. Hum. Genet.* **2020**, *28*, 165–173. [CrossRef]
7. Gorini, F.; Coi, A.; Mezzasalma, L.; Baldacci, S.; Pierini, A.; Santoro, M. Survival of Patients with Rare Diseases: A Population-Based Study in Tuscany (Italy). *Orphanet J. Rare Dis.* **2021**, *16*, 275. [CrossRef]
8. Yoo, H.W. Development of Orphan Drugs for Rare Diseases. *Clin. Exp. Pediatr.* **2024**, *67*, 315–327. [CrossRef]
9. Abozaid, G.M.; Kerr, K.; McKnight, A.; Al-Omar, H.A. Criteria to Define Rare Diseases and Orphan Drugs: A Systematic Review Protocol. *BMJ Open* **2022**, *12*, e062126. [CrossRef]
10. Waxman, H. H.R. 5238—97th Congress (1981–1982): Orphan Drug Act. 1983. Available online: <https://www.congress.gov/bill/97th-congress/house-bill/5238/summary/00> (accessed on 21 August 2024).
11. McNeilly, E.K. Designating an Orphan Product: Drug and Biological Products—Orphan Drug Regulations: Regulatory History. Available online: <https://www.fda.gov/industry/medical-products-rare-diseases-and-conditions/designating-orphan-product-drugs-and-biological-products> (accessed on 21 August 2024).
12. Tsuboi, Y.; Mishima, T.; Fujioka, S. Perry Disease: Concept of a New Disease and Clinical Diagnostic Criteria. *J. Mov. Disord.* **2021**, *14*, 1–9. [CrossRef]

13. Perry, T.L.; Bratty, P.J.A.; Hansen, S.; Kennedy, J.; Urquhart, N.; Dolman, C.L. Hereditary Mental Depression and Parkinsonism With Taurine Deficiency. *Arch. Neurol.* **1975**, *32*, 108–113. [[CrossRef](#)] [[PubMed](#)]
14. Mishima, T.; Yuasa-Kawada, J.; Fujioka, S.; Tsuboi, Y. Perry Disease: Bench to Bedside Circulation and a Team Approach. *Biomedicines* **2024**, *12*, 113. [[CrossRef](#)] [[PubMed](#)]
15. Dulski, J.; Cerquera-Cleves, C.; Milanowski, L.; Kidd, A.; Sitek, E.J.; Strongosky, A.; Vanegas Monroy, A.M.; Dickson, D.W.; Ross, O.A.; Pentela-Nowicka, J.; et al. Clinical, Pathological and Genetic Characteristics of Perry Disease—New Cases and Literature Review. *Eur. J. Neurol.* **2021**, *28*, 4010–4021. [[CrossRef](#)] [[PubMed](#)]
16. Dulski, J.; Cerquera-Cleves, C.; Milanowski, L.; Kwiatek-Majkusiak, J.; Kozirowski, D.; Ross, O.A.; Pentela-Nowicka, J.; Sławek, J.; Wszolek, Z.K. L-Dopa Response, Choreic Dyskinesia, and Dystonia in Perry Syndrome. *Park. Relat. Disord.* **2022**, *100*, 19–23. [[CrossRef](#)]
17. Wider, C.; Wszolek, Z.K. Rapidly Progressive Familial Parkinsonism with Central Hypoventilation, Depression and Weight Loss (Perry Syndrome)—A Literature Review. *Park. Relat. Disord.* **2008**, *14*, 1–7. [[CrossRef](#)]
18. Milanowski, L.; Sitek, E.J.; Dulski, J.; Cerquera-Cleves, C.; Gomez, J.D.; Brockhuis, B.; Schinwelski, M.; Kluj-Kozłowska, K.; Ross, O.A.; Sławek, J.; et al. Cognitive and Behavioral Profile of Perry Syndrome in Two Families. *Park. Relat. Disord.* **2020**, *77*, 114–120. [[CrossRef](#)]
19. Dulski, J.; Koga, S.; Liberski, P.P.; Sitek, E.J.; Butala, A.A.; Sławek, J.; Dickson, D.W.; Wszolek, Z.K. Perry Disease: Expanding the Genetic Basis. *Mov. Disord. Clin. Pract.* **2023**, *10*, 1136–1142. [[CrossRef](#)]
20. Stoker, T.B.; Dostal, V.; Cochius, J.; Williams-Gray, C.H.; Scherzer, C.R.; Wang, J.; Liu, G.; Coyle-Gilchrist, I. DCTN1 Mutation Associated Parkinsonism: Case Series of Three New Families with Perry Syndrome. *J. Neurol.* **2022**, *269*, 6667–6672. [[CrossRef](#)]
21. Silva, E.; Itzcovich, T.; Niikado, M.; Caride, A.; Fernández, E.; Vázquez, J.C.; Romorini, L.; Marazita, M.; Sevlever, G.; Martinetto, H.; et al. Perry Disease in an Argentine Family Due to the DCTN1 p.G67D Variant. *Park. Relat. Disord.* **2022**, *97*, 63–64. [[CrossRef](#)]
22. Dixon, S.L.; Smondyrev, A.M.; Rao, S.N. PHASE: A Novel Approach to Pharmacophore Modeling and 3D Database Searching. *Chem. Biol. Drug Des.* **2006**, *67*, 370–372. [[CrossRef](#)]
23. Dixon, S.L.; Smondyrev, A.M.; Knoll, E.H.; Rao, S.N.; Shaw, D.E.; Friesner, R.A. PHASE: A New Engine for Pharmacophore Perception, 3D QSAR Model Development, and 3D Database Screening: 1. Methodology and Preliminary Results. *J. Comput. Aided Mol. Des.* **2006**, *20*, 647–671. [[CrossRef](#)] [[PubMed](#)]
24. Berman, H.M.; Westbrook, J.; Feng, Z.; Gilliland, G.; Bhat, T.N.; Weissig, H.; Shindyalov, I.N.; Bourne, P.E. The Protein Data Bank. *Nucleic Acids Res.* **2000**, *28*, 235–242. [[CrossRef](#)] [[PubMed](#)]
25. Zdrzil, B.; Felix, E.; Hunter, F.; Manners, E.J.; Blackshaw, J.; Corbett, S.; de Veij, M.; Ioannidis, H.; Lopez, D.M.; Mosquera, J.F.; et al. The ChEMBL Database in 2023: A Drug Discovery Platform Spanning Multiple Bioactivity Data Types and Time Periods. *Nucleic Acids Res.* **2024**, *52*, D1180–D1192. [[CrossRef](#)] [[PubMed](#)]
26. Mendez, D.; Gaulton, A.; Bento, A.P.; Chambers, J.; De Veij, M.; Félix, E.; Magariños, M.P.; Mosquera, J.F.; Mutowo, P.; Nowotka, M.; et al. ChEMBL: Towards Direct Deposition of Bioassay Data. *Nucleic Acids Res.* **2019**, *47*, D930–D940. [[CrossRef](#)]
27. Binda, C.; Wang, J.; Pisani, L.; Caccia, C.; Carotti, A.; Salvati, P.; Edmondson, D.E.; Mattevi, A. Structures of Human Monoamine Oxidase B Complexes with Selective Noncovalent Inhibitors: Safinamide and Coumarin Analogs. *J. Med. Chem.* **2007**, *50*, 5848–5852. [[CrossRef](#)]
28. Coleman, J.A.; Gouaux, E. Structural Basis for Recognition of Diverse Antidepressants by the Human Serotonin Transporter. *Nat. Struct. Mol. Biol.* **2018**, *25*, 170–175. [[CrossRef](#)]
29. Xu, P.; Huang, S.; Krumm, B.E.; Zhuang, Y.; Mao, C.; Zhang, Y.; Wang, Y.; Huang, X.P.; Liu, Y.F.; He, X.; et al. Structural Genomics of the Human Dopamine Receptor System. *Cell Res.* **2023**, *33*, 604–616. [[CrossRef](#)]
30. Xu, P.; Huang, S.; Zhang, H.; Mao, C.; Zhou, X.E.; Cheng, X.; Simon, I.A.; Shen, D.D.; Yen, H.Y.; Robinson, C.V.; et al. Structural Insights into the Lipid and Ligand Regulation of Serotonin Receptors. *Nature* **2021**, *592*, 469–473. [[CrossRef](#)]
31. Finberg, J.P.M.; Rabey, J.M. Inhibitors of MAO-A and MAO-B in Psychiatry and Neurology. *Front. Pharmacol.* **2016**, *7*, 340. [[CrossRef](#)]
32. Baweja, G.S.; Gupta, S.; Kumar, B.; Patel, P.; Asati, V. Recent Updates on Structural Insights of MAO-B Inhibitors: A Review on Target-Based Approach. *Mol. Divers.* **2023**, *28*, 1823–1845. [[CrossRef](#)]
33. Novaroli, L.; Reist, M.; Favre, E.; Carotti, A.; Catto, M.; Carrupt, P.A. Human Recombinant Monoamine Oxidase B as Reliable and Efficient Enzyme Source for Inhibitor Screening. *Bioorg. Med. Chem.* **2005**, *13*, 6212–6217. [[CrossRef](#)] [[PubMed](#)]
34. Tan, Y.Y.; Jenner, P.; Chen, S. Di Monoamine Oxidase-B Inhibitors for the Treatment of Parkinson’s Disease: Past, Present, and Future. *J. Park. Dis.* **2022**, *12*, 477–493. [[CrossRef](#)]
35. Evren, A.E.; Nuha, D.; Dawbaa, S.; Sağlık, B.N.; Yurttaş, L. Synthesis of Novel Thiazolyl Hydrazone Derivatives as Potent Dual Monoamine Oxidase-Aromatase Inhibitors. *Eur. J. Med. Chem.* **2022**, *229*, 114097. [[CrossRef](#)] [[PubMed](#)]
36. Grychowska, K.; Olejarz-Maciej, A.; Blicharz, K.; Pietruś, W.; Karcz, T.; Kurczab, R.; Koczurkiewicz, P.; Doroz-Płonka, A.; Latacz, G.; Keeri, A.R.; et al. Overcoming Undesirable HERG Affinity by Incorporating Fluorine Atoms: A Case of MAO-B Inhibitors Derived from 1 H-Pyrrolo-[3,2-c]Quinolines. *Eur. J. Med. Chem.* **2022**, *236*, 114329. [[CrossRef](#)]
37. Paolino, M.; Rullo, M.; Maramai, S.; de Candia, M.; Pisani, L.; Catto, M.; Mugnaini, C.; Brizzi, A.; Cappelli, A.; Olivucci, M.; et al. Design, Synthesis and Biological Evaluation of Light-Driven on-off Multitarget AChE and MAO-B Inhibitors. *RSC Med. Chem.* **2022**, *13*, 873–883. [[CrossRef](#)]

38. Jin, C.F.; Wang, Z.Z.; Chen, K.Z.; Xu, T.F.; Hao, G.F. Computational Fragment-Based Design Facilitates Discovery of Potent and Selective Monoamine Oxidase-B (MAO-B) Inhibitor. *J. Med. Chem.* **2020**, *63*, 15021–15036. [[CrossRef](#)]
39. Wang, Z.; Yi, C.; Chen, K.; Wang, T.; Deng, K.; Jin, C.; Hao, G. Enhancing Monoamine Oxidase B Inhibitory Activity via Chiral Fluorination: Structure-Activity Relationship, Biological Evaluation, and Molecular Docking Study. *Eur. J. Med. Chem.* **2022**, *228*, 114025. [[CrossRef](#)]
40. Kong, H.; Meng, X.; Hou, R.; Yang, X.; Han, J.; Xie, Z.; Duan, Y.; Liao, C. Novel 1-(Prop-2-Yn-1-Ylamino)-2,3-Dihydro-1H-Indene-4-Thiol Derivatives as Potent Selective Human Monoamine Oxidase B Inhibitors: Design, SAR Development, and Biological Evaluation. *Bioorg. Med. Chem. Lett.* **2021**, *43*, 128051. [[CrossRef](#)]
41. López-Echeverri, Y.P.; Cardona-Londoño, K.J.; Garcia-Aguirre, J.F.; Orrego-Cardozo, M. Effects of Serotonin Transporter and Receptor Polymorphisms on Depression. *Rev. Colomb. Psiquiatr. (Engl. Ed.)* **2023**, *52*, 130–138. [[CrossRef](#)]
42. Haney, E.M.; Calarge, C.; Bliziotis, M.M. Clinical Implications of Serotonin Regulation of Bone Mass. In *Translational Endocrinology of Bone: Reproduction, Metabolism, and the Central Nervous System*; Elsevier: Amsterdam, The Netherlands, 2012; pp. 189–198. [[CrossRef](#)]
43. Singh, I.; Seth, A.; Billesbølle, C.B.; Braz, J.; Rodriguiz, R.M.; Roy, K.; Bekele, B.; Craik, V.; Huang, X.P.; Boytsov, D.; et al. Structure-Based Discovery of Conformationally Selective Inhibitors of the Serotonin Transporter. *Cell* **2023**, *186*, 2160–2175.e17. [[CrossRef](#)]
44. Politis, M.; Loane, C. Serotonergic Dysfunction in Parkinson's Disease and Its Relevance to Disability. *Sci. World J.* **2011**, *11*, 1726–1734. [[CrossRef](#)] [[PubMed](#)]
45. Sid-Otmane, L.; Huot, P.; Panisset, M. Effect of Antidepressants on Psychotic Symptoms in Parkinson Disease: A Review of Case Reports and Case Series. *Clin. Neuropharmacol.* **2020**, *43*, 61–65. [[CrossRef](#)] [[PubMed](#)]
46. Manepalli, S.; Geffert, L.M.; Surratt, C.K.; Madura, J.D. Discovery of Novel Selective Serotonin Reuptake Inhibitors through Development of a Protein-Based Pharmacophore. *J. Chem. Inf. Model.* **2011**, *51*, 2417–2426. [[CrossRef](#)] [[PubMed](#)]
47. Ye, N.; Qin, W.; Tian, S.; Xu, Q.; Wold, E.A.; Zhou, J.; Zhen, X.C. Small Molecules Selectively Targeting Sigma-1 Receptor for the Treatment of Neurological Diseases. *J. Med. Chem.* **2020**, *63*, 15187–15217. [[CrossRef](#)]
48. Sorrentino, J.P.; Altman, R.A. Fluoroalkylation of Dextromethorphan Improves CNS Exposure and Metabolic Stability. *ACS Med. Chem. Lett.* **2022**, *13*, 707–713. [[CrossRef](#)]
49. Zhang, C.; Wang, L.; Xu, Y.; Huang, Y.; Huang, J.; Zhu, J.; Wang, W.; Li, W.; Sun, A.; Li, X.; et al. Discovery of Novel Dual RAGE/SERT Inhibitors for the Potential Treatment of the Comorbidity of Alzheimer's Disease and Depression. *Eur. J. Med. Chem.* **2022**, *236*, 114347. [[CrossRef](#)]
50. Li, X.; Li, J.; Huang, Y.; Gong, Q.; Fu, Y.; Xu, Y.; Huang, J.; You, H.; Zhang, D.; Zhang, D.; et al. The Novel Therapeutic Strategy of Vilazodone-Donepezil Chimeras as Potent Triple-Target Ligands for the Potential Treatment of Alzheimer's Disease with Comorbid Depression. *Eur. J. Med. Chem.* **2022**, *229*, 114045. [[CrossRef](#)]
51. Kargbo, R.B. Ibogaine and Their Analogs as Therapeutics for Neurological and Psychiatric Disorders. *ACS Med. Chem. Lett.* **2022**, *13*, 888–890. [[CrossRef](#)]
52. Yuan, S.; Yu, B.; Liu, H.M. New Drug Approvals for 2019: Synthesis and Clinical Applications. *Eur. J. Med. Chem.* **2020**, *205*, 112667. [[CrossRef](#)]
53. Kverno, K. Dextromethorphan From Cough Suppressant to Antidepressant. *J. Psychosoc. Nurs. Ment. Health Serv.* **2022**, *60*, 9–11. [[CrossRef](#)]
54. Fox, S.H.; Metman, L.V.; Nutt, J.G.; Brodsky, M.; Factor, S.A.; Lang, A.E.; Pope, L.E.; Knowles, N.; Siffert, J. Trial of Dextromethorphan/Quinidine to Treat Levodopa-Induced Dyskinesia in Parkinson's Disease. *Mov. Disord.* **2017**, *32*, 893–903. [[CrossRef](#)] [[PubMed](#)]
55. Nguyen, L.; Thomas, K.L.; Lucke-Wold, B.P.; Cavendish, J.Z.; Crowe, M.S.; Matsumoto, R.R. Dextromethorphan: An Update on Its Utility for Neurological and Neuropsychiatric Disorders. *Pharmacol. Ther.* **2016**, *159*, 1–22. [[CrossRef](#)] [[PubMed](#)]
56. Khoury, R. Deuterated Dextromethorphan/Quinidine for Agitation in Alzheimer's Disease. *Neural Regen. Res.* **2022**, *17*, 1013–1014. [[CrossRef](#)] [[PubMed](#)]
57. Chen, C.Y.; Chung, C.H.; Chien, W.C.; Chen, H.C. The Association between Dextromethorphan Use and the Risk of Dementia. *Am. J. Alzheimers Dis. Other Dement.* **2022**, *37*, 153331752211249. [[CrossRef](#)]
58. Popik, P.; Skolnick, P. Chapter 3 Pharmacology of Ibogaine And Ibogaine-Related Alkaloids. *Alkaloids Chem. Biol.* **1999**, *52*, 197–231. [[CrossRef](#)]
59. Iyer, R.N.; Favela, D.; Zhang, G.; Olson, D.E. The Iboga Enigma: The Chemistry and Neuropharmacology of Iboga Alkaloids and Related Analogs. *Nat. Prod. Rep.* **2021**, *38*, 307–329. [[CrossRef](#)]
60. Latif, S.; Jahangeer, M.; Maknoon Razia, D.; Ashiq, M.; Ghaffar, A.; Akram, M.; El Allam, A.; Bouyahya, A.; Garipova, L.; Ali Shariati, M.; et al. Dopamine in Parkinson's Disease. *Clin. Chim. Acta* **2021**, *522*, 114–126. [[CrossRef](#)]
61. Juza, R.; Musilek, K.; Mezeiova, E.; Soukup, O.; Korabecny, J. Recent Advances in Dopamine D2 Receptor Ligands in the Treatment of Neuropsychiatric Disorders. *Med. Res. Rev.* **2023**, *43*, 55–211. [[CrossRef](#)]
62. Cacabelos, R. Parkinson's Disease: From Pathogenesis to Pharmacogenomics. *Int. J. Mol. Sci.* **2017**, *18*, 551. [[CrossRef](#)]
63. Suski, V.; Stacy, M. Dopamine Agonists. In *Handbook Parkinson's Disease*, 5th ed.; Jaypee: New Delhi, India, 2013; pp. 414–429. [[CrossRef](#)]

64. Ooba, N.; Yamaguchi, T.; Kubota, K. The Impact in Japan of Regulatory Action on Prescribing of Dopamine Receptor Agonists: Analysis of a Claims Database between 2005 and 2008. *Drug Saf.* **2011**, *34*, 329–338. [[CrossRef](#)]
65. Isaacson, S.H.; Hauser, R.A.; Pahwa, R.; Gray, D.; Duvvuri, S. Dopamine Agonists in Parkinson's Disease: Impact of D1-like or D2-like Dopamine Receptor Subtype Selectivity and Avenues for Future Treatment. *Clin. Park. Relat. Disord.* **2023**, *9*, 100212. [[CrossRef](#)] [[PubMed](#)]
66. Park, H.; Urs, A.N.; Zimmerman, J.; Liu, C.; Wang, Q.; Urs, N.M. Structure-Functional-Selectivity Relationship Studies of Novel Apomorphine Analogs to Develop D1R/D2R Biased Ligands. *ACS Med. Chem. Lett.* **2020**, *11*, 385–392. [[CrossRef](#)] [[PubMed](#)]
67. Yan, W.; Fan, L.; Yu, J.; Liu, R.; Wang, H.; Tan, L.; Wang, S.; Cheng, J. 2-Phenylcyclopropylmethylamine Derivatives as Dopamine D2 Receptor Partial Agonists: Design, Synthesis, and Biological Evaluation. *J. Med. Chem.* **2021**, *64*, 17239–17258. [[CrossRef](#)]
68. Tropmann, K.; Bresinsky, M.; Forster, L.; Mönnich, D.; Buschauer, A.; Wittmann, H.J.; Hübner, H.; Gmeiner, P.; Pockes, S.; Strasser, A. Abolishing Dopamine D2long/D3 Receptor Affinity of Subtype-Selective Carbamoylguanidine-Type Histamine H2 Receptor Agonists. *J. Med. Chem.* **2021**, *64*, 8684–8709. [[CrossRef](#)] [[PubMed](#)]
69. Dinda, B.; Das, B.; Biswas, S.; Sharma, H.; Armstrong, C.; Yedlapudi, D.; Antonio, T.; Reith, M.; Dutta, A.K. Bivalent Dopamine Agonists with Co-Operative Binding and Functional Activities at Dopamine D2 Receptors, Modulate Aggregation and Toxicity of Alpha Synuclein Protein. *Bioorg. Med. Chem.* **2023**, *78*, 117131. [[CrossRef](#)]
70. Qian, M.; Ricarte, A.; Wouters, E.; Dalton, J.A.R.; Risseuw, M.D.P.; Giraldo, J.; Van Calenbergh, S. Discovery of a True Bivalent Dopamine D2 Receptor Agonist. *Eur. J. Med. Chem.* **2021**, *212*, 113151. [[CrossRef](#)]
71. Zhong, Z.; He, X.; Ge, J.; Zhu, J.; Yao, C.; Cai, H.; Ye, X.Y.; Xie, T.; Bai, R. Discovery of Small-Molecule Compounds and Natural Products against Parkinson's Disease: Pathological Mechanism and Structural Modification. *Eur. J. Med. Chem.* **2022**, *237*, 114378. [[CrossRef](#)]
72. Gogoi, S.; Biswas, S.; Modi, G.; Antonio, T.; Reith, M.E.A.; Dutta, A.K. Novel Bivalent Ligands for D2/D3 Dopamine Receptors: Significant Cooperative Gain in D2 Affinity and Potency. *ACS Med. Chem. Lett.* **2012**, *3*, 991–996. [[CrossRef](#)]
73. Eremin, D.V.; Kondaurova, E.M.; Rodnyy, A.Y.; Molobekova, C.A.; Kudlay, D.A.; Naumenko, V.S. Serotonin Receptors as a Potential Target in the Treatment of Alzheimer's Disease. *Biochemistry* **2023**, *88*, 2023–2042. [[CrossRef](#)]
74. Pytliak, M.; Vargová, V.; Mechírová, V.; Felšci, M. Serotonin Receptors—From Molecular Biology to Clinical Applications. *Physiol. Res.* **2011**, *60*, 15–25. [[CrossRef](#)]
75. Żmudzka, E.; Sałaciak, K.; Sapa, J.; Pytka, K. Serotonin Receptors in Depression and Anxiety: Insights from Animal Studies. *Life Sci.* **2018**, *210*, 106–124. [[CrossRef](#)] [[PubMed](#)]
76. Jaronczyk, M.; Walory, J. Novel Molecular Targets of Antidepressants. *Molecules* **2022**, *27*, 533. [[CrossRef](#)] [[PubMed](#)]
77. Zagórska, A.; Bucki, A.; Partyka, A.; Jastrzębska-Więsek, M.; Siwek, A.; Głuch-Lutwin, M.; Mordyl, B.; Jaromin, A.; Walczak, M.; Wesołowska, A.; et al. Design, Synthesis, and Behavioral Evaluation of Dual-Acting Compounds as Phosphodiesterase Type 10A (PDE10A) Inhibitors and Serotonin Ligands Targeting Neuropsychiatric Symptoms in Dementia. *Eur. J. Med. Chem.* **2022**, *233*, 114218. [[CrossRef](#)] [[PubMed](#)]
78. Tan, X.; Jiang, X.; He, Y.; Zhong, F.; Li, X.; Xiong, Z.; Li, Z.; Liu, X.; Cui, C.; Zhao, Q.; et al. Automated Design and Optimization of Multitarget Schizophrenia Drug Candidates by Deep Learning. *Eur. J. Med. Chem.* **2020**, *204*, 112572. [[CrossRef](#)]
79. Shi, W.; Wang, Y.; Wu, C.; Yang, F.; Zheng, W.; Wu, S.; Liu, Y.; Wang, Z.; He, Y.; Shen, J. Synthesis and Biological Investigation of Triazolopyridinone Derivatives as Potential Multireceptor Atypical Antipsychotics. *Bioorg. Med. Chem. Lett.* **2020**, *30*, 127027. [[CrossRef](#)]
80. Schrödinger. *Release 2024-2: Maestro*; Schrödinger, LLC: New York, NY, USA, 2024.
81. Schrödinger. *Release 2024-2: Protein Preparation Wizard*; Epik, Schrödinger, LLC: New York, NY, USA; Impact, Schrödinger, LLC: New York, NY, USA; Prime, Schrödinger, LLC: New York, NY, USA, 2024.
82. Madhavi Sastry, G.; Adzhigirey, M.; Day, T.; Annabhimoju, R.; Sherman, W. Protein and Ligand Preparation: Parameters, Protocols, and Influence on Virtual Screening Enrichments. *J. Comput. Aided Mol. Des.* **2013**, *27*, 221–234. [[CrossRef](#)]
83. Schrödinger. *Release 2024-2: LigPrep*; Schrödinger, LLC: New York, NY, USA, 2024.
84. Schrödinger. *Release 2024-2: Phase*; Schrödinger, LLC: New York, NY, USA, 2024.
85. Singh, S.; Gupta, H.; Sharma, P.; Sahi, S. Advances in Artificial Intelligence (AI)-Assisted Approaches in Drug Screening. *Artif. Intell. Chem.* **2024**, *2*, 100039. [[CrossRef](#)]
86. Cichońska, A.; Ravikumar, B.; Rahman, R. AI for Targeted Polypharmacology: The next Frontier in Drug Discovery. *Curr. Opin. Struct. Biol.* **2024**, *84*, 102771. [[CrossRef](#)]
87. Singh, N.; Vayer, P.; Tanwar, S.; Poyet, J.-L.; Tsaioun, K.; Villoutreix, B.O. Drug Discovery and Development: Introduction to the General Public and Patient Groups. *Front. Drug Discov.* **2023**, *3*, 1201419. [[CrossRef](#)]
88. Berdigaliyev, N.; Aljofan, M. An Overview of Drug Discovery and Development. *Future Med. Chem.* **2020**, *12*, 939–947. [[CrossRef](#)]

Disclaimer/Publisher's Note: The statements, opinions and data contained in all publications are solely those of the individual author(s) and contributor(s) and not of MDPI and/or the editor(s). MDPI and/or the editor(s) disclaim responsibility for any injury to people or property resulting from any ideas, methods, instructions or products referred to in the content.